

# Symmetry energy of cold nucleonic matter within a relativistic mean field model encapsulating effects of high momentum nucleons induced by short-range correlations

Bao-Jun Cai<sup>\*1</sup> and Bao-An Li<sup>†1</sup>

<sup>1</sup>*Department of Physics and Astronomy, Texas A&M University-Commerce, Commerce, TX 75429-3011, USA*

(Dated: January 18, 2016)

It is well known that short-range nucleon-nucleon correlations (SRC) due to the tensor components and/or the repulsive core of nuclear forces lead to a high (low) momentum tail (depletion) in the single-nucleon momentum distribution above (below) the nucleon Fermi surface in cold nucleonic matter. Significant progress has been made recently in constraining the isospin-dependent parameters characterizing the SRC-modified single-nucleon momentum distribution in neutron-rich nucleonic matter using both experimental data and microscopic model calculations. Using the constrained single-nucleon momentum distribution in a nonlinear relativistic mean field (RMF) model, we study the equation of state (EOS) of asymmetric nucleonic matter (ANM), especially the density dependence of nuclear symmetry energy  $E_{\text{sym}}(\rho)$ . Firstly, as a test of the model, the average nucleon kinetic energy extracted recently from electron-nucleus scattering experiments using a neutron-proton dominance model is well reproduced by the RMF model incorporating effects of the SRC-induced high momentum nucleons, while it is significantly under predicted by the RMF model using a step function for the single-nucleon momentum distribution as in free Fermi gas (FFG) models. Secondly, consistent with earlier findings within non-relativistic models, the kinetic symmetry energy of quasi-nucleons is found to be  $E_{\text{sym}}^{\text{kin}}(\rho_0) = -16.94 \pm 13.66$  MeV which is dramatically different from the prediction of  $E_{\text{sym}}^{\text{kin}}(\rho_0) \approx 12.5$  MeV by FFG models at nuclear matter saturation density  $\rho_0 = 0.16 \text{ fm}^{-3}$ . Thirdly, comparing the RMF calculations with and without the high momentum nucleons using two sets of model parameters both reproducing identically all empirically constraints on the EOS of symmetric nuclear matter (SNM) and the symmetry energy of ANM at  $\rho_0$ , the SRC-modified single-nucleon momentum distribution is found to make the  $E_{\text{sym}}(\rho)$  more concave around  $\rho_0$  by softening it significantly at both sub-saturation and supra-saturation densities, leading to an isospin-dependent incompressibility of ANM in better agreement with existing experimental data. Fourthly, the maximum mass of neutron stars is enhanced by the increased kinetic pressure from high-momentum nucleons at supra-saturation densities in SNM.

PACS numbers: 21.65.Ef, 24.10.Ht, 21.65.Cd

## I. INTRODUCTION

The density dependence of nuclear symmetry  $E_{\text{sym}}(\rho)$  is currently the most uncertain part of the equation of state (EOS) of isospin asymmetric nucleonic matter (ANM) especially at supra-saturation densities [1]. Owing to its importance in both nuclear physics [2–9] and astrophysics [10–13], much efforts have been devoted in recent years to constraining the  $E_{\text{sym}}(\rho)$  using data from both terrestrial experiments and astrophysical observations [1]. While significant progress has been made in experimentally constraining the  $E_{\text{sym}}(\rho)$  around the saturation density  $\rho_0$ , much more work is needed to better constrain the  $E_{\text{sym}}(\rho)$  at both sub-saturation and supra-saturation densities. On the other hand, essentially all existing nuclear interactions have been used in various many-body theories to calculate the  $E_{\text{sym}}(\rho)$ . While all models are tuned to be consistent with available constraints on the  $E_{\text{sym}}(\rho)$  around  $\rho_0$ , their predictions diverge broadly at supra-saturation densities. For uniform nucleonic matter, extensive studies have been un-

derway by various groups to understand why the  $E_{\text{sym}}(\rho)$  is so uncertain especially at high densities and how one can better constrain it. The spin-isospin dependence of three-body forces and the isospin dependence of short-range nucleon-nucleon correlations (SRC) induced by the poorly known nuclear tensor forces and the repulsive core have been identified in several studies to be among the main causes of the uncertainties in the  $E_{\text{sym}}(\rho)$  at supra-saturation densities, see, e.g., refs. [14–17]. While at very low densities where cluster formation and pairing become important, the  $E_{\text{sym}}(\rho)$  behaves rather differently from expectations based on mean-field models [18–20]. Moreover, for clustered matter where correlations dominate and the Coulomb force is important, there is no neutron-proton exchange symmetry, it is even a question whether it is necessary and how to introduce the symmetry energy in describing the EOS of clustered matter.

How to relate isovector interactions with experimental observables sensitive to the  $E_{\text{sym}}(\rho)$  has been a longstanding question [1]. A thorough understanding about the origins and properties of each part of the  $E_{\text{sym}}(\rho)$  is useful for making further progress in this field. Usually, the symmetry energy  $E_{\text{sym}}(\rho)$  can be decomposed into a kinetic and a potential part, i.e.,  $E_{\text{sym}}(\rho) = E_{\text{sym}}^{\text{kin}}(\rho) + E_{\text{sym}}^{\text{pot}}(\rho)$ . We emphasize that such a decomposition should be understood as for quasi-nucleons of cer-

<sup>\*</sup>Email: landau1908feynman1918@gmail.com

<sup>†</sup>Corresponding author: Bao-An.Li@tamuc.edu

tain effective masses and momentum distributions which are both determined by nuclear interactions. Namely, the kinetic symmetry energy of quasi-nucleons also depends on the interaction. However, in many analyses of data especially using phenomenological models one often assumes that the kinetic symmetry energy is that predicted by the free Fermi gas (FFG) model for nucleons with bare masses and step functions for their momentum distributions. The potential part is often parameterized with its parameters extracted from fitting the data within adopted models for describing the physics in question.

It is well known that short-range nucleon-nucleon correlations due to the tensor components and/or the repulsive core of nuclear forces lead to a high (low) momentum tail (depletion) in the single-nucleon momentum distribution above (below) the nucleon Fermi surface in cold nucleonic matter, see, e.g., refs. [21–24] for comprehensive reviews. In recent years, significant efforts have been made, e.g., refs. [25–30], to constrain the isospin-dependent parameters characterizing the SRC-modified single-nucleon momentum distribution in neutron-rich nucleonic matter using both experimental data and microscopic model calculations. For instance, it has been found from analyzing electron-nucleus scattering data that the percentage of nucleons in the high momentum tail (HMT) above the Fermi surface is as high as about 25% in symmetric nuclear matter (SNM) but decreases gradually to about only 1% in pure neutron matter (PNM) [27, 28]. Thus, the SRC-modified quasi-nucleon momentum distribution is significantly different from the step function for the FFG at zero temperature. Because of the momentum-squared weighting in calculating the average nucleon kinetic energy, the strong isospin dependence of the HMT makes the kinetic symmetry energy dramatically different from the FFG model prediction using a step function for the nucleon momentum distribution [31–39]. In particular, the kinetic symmetry energy is significantly reduced to even negative values in some model studies. In essence, the symmetry energy is the energy difference between PNM and SNM in the parabolic approximation of the ANM EOS. The neutron-proton interaction dominated SRC increases significantly the average energy per nucleon in SNM but has little effect on that in PNM, thus leading to a reduction of the kinetic symmetry energy. This expectation has been confirmed so far only within non-relativistic approaches. It would be interesting to study effects of the HMT on both the kinetic and potential parts of the  $E_{\text{sym}}(\rho)$  within a relativistic model.

The knowledge on each individual term of the  $E_{\text{sym}}(\rho)$  is useful in both nuclear physics and astrophysics. For instance, in simulating heavy-ion reactions using transport models one needs as an input the potential symmetry energy of quasi-nucleons. Its magnitude is limited by the total symmetry energy at  $\rho_0$  known to be around  $31.6 \pm 2.66$  MeV [40] and the kinetic symmetry energy normally assumed to be that predicted by the FFG model. Several recent studies have shown that using a SRC-reduced ki-

netic symmetry energy in transport model simulations can lead to significant effects on isovector observables of heavy-ion collisions [38, 41–43]. Interestingly, it was also found recently that the critical densities and effects of the formation of different charge states of  $\Delta(1232)$  resonances in neutron stars depend on how the kinetic and potential parts of the  $E_{\text{sym}}(\rho)$  individually evolve as functions of density [44, 45]. Namely, in determining the critical formation densities for  $\Delta(1232)$  resonances in neutron stars using chemical equilibrium conditions, the kinetic and potential parts of the nucleon symmetry energy play different roles [44]. Basically, the  $\Delta(1232)$  resonances obtain a potential symmetry energy due to the  $\tau_3(\Delta) \cdot \tau_3(N)$  term in their interactions with nucleons where the  $\tau_3(\Delta)$  and  $\tau_3(N)$  are the third component of the isospin of  $\Delta$  resonances and nucleons. However, the population of  $\Delta$  resonances is so low especially near their production thresholds that they do not built their own Fermi spheres and thus they do not have a kinetic symmetry energy. Depending on the relative strengths of the  $NN\rho$  and  $\Delta\Delta\rho$  coupling constants  $g_{\rho N}$  and  $g_{\rho\Delta}$ , the potential symmetry energies of the  $\Delta$  resonances and nucleons may completely cancel out but the kinetic symmetry energy of nucleons remains in the equations determining the critical formation densities of the four charge states of  $\Delta$  resonances [44].

In this work, within a nonlinear relativistic mean field (RMF) model incorporating the SRC-modified single-nucleon momentum distribution with its parameters determined by electron-nucleus scattering experiments and calculations using state-of-the-art many-body theories, we study the EOS of ANM especially the  $E_{\text{sym}}(\rho)$ . Several interesting effects are found. In particular, comparing the RMF calculations with and without the HMT using two sets of model parameters both reproducing identically all empirically constraints on the EOS of SNM and the symmetry energy of ANM at  $\rho_0$ , the SRC-modified nucleon momentum distribution leads to a negative kinetic symmetry energy and the total symmetry energy is softened at both sub-saturation and supra-saturation densities. Moreover, only with the SRC-modified nucleon momentum distribution, the recently extracted average kinetic energy per nucleon from electron-nucleus scattering experiments can be reproduced, providing a strong support for the existence of HMT in nuclei. Furthermore, the HMT also enhance the maximum mass of neutron stars by increasing the kinetic pressure of SNM at supra-saturation densities.

The paper is organized as follows, in Section II, the SRC-modified single-nucleon momentum distribution with a HMT and the basic equations of the nonlinear RMF model are outlined. In Section III, we evaluate the kinetic symmetry energy with the SRC-modified single nucleon momentum distribution. Effects on the EOS of SNM and the validation of the HMT are presented in Section IV. In Section V, effects of the HMT on the nucleon scalar density and Dirac effective mass are studied. Then in Section VI we examine effects of the HMT on

the density dependence of the total symmetry energy. In Section VII, the effects of the HMT on the EOS of neutron star matter as well as the mass-radius relation of neutron stars will be explored. Finally, we summarize in Section VIII. Detailed derivations for the analytical expressions of the kinetic symmetry energy, incompressibility coefficient  $K_0$  of SNM and the slope parameter  $L$  of the symmetry energy within the RMF with HMT are given in the three Appendixes.

## II. A RELATIVISTIC MEAN FIELD MODEL INCORPORATING THE SRC-MODIFIED NUCLEON MOMENTUM DISTRIBUTION

In this section, we first summarize the main features and give all parameters of the SRC-modified single-nucleon momentum distribution. Then we discuss how the relevant formalisms of the nonlinear RMF model are generalized by replacing the previously used step function for the nucleon momentum distribution with the SRC-modified one including a high-momentum tail. We notice that tensor forces have no effect at the mean-field level. The SRC-modified momentum distribution can not be obtained self-consistently within the RMF model itself.

### A. The SRC-Modified Nucleon Momentum Distribution Function

Here we briefly describe the SRC-modified single-nucleon momentum distribution function encapsulating a high momentum tail used in the present work. More details can be found in ref. [39]. The single-nucleon momentum distribution function in ANM has the following form,

$$n_{\mathbf{k}}^J(\rho, \delta) = \begin{cases} \Delta_J + \beta_J I(|\mathbf{k}|/k_F^J), & 0 < |\mathbf{k}| < k_F^J, \\ C_J (k_F^J/|\mathbf{k}|)^4, & k_F^J < |\mathbf{k}| < \phi_J k_F^J. \end{cases} \quad (1)$$

Here,  $J = n, p$  is the isospin index,  $k_F^J = k_F(1 + \tau_3^J \delta)^{1/3}$  is the Fermi momentum where  $k_F = (3\pi^2 \rho/2)^{1/3}$  and  $\tau_3^n = +1$ ,  $\tau_3^p = -1$ . It is worth emphasizing that the above form of nucleon momentum distribution function is consistent with the well-known predictions of microscopic nuclear many-body theories [21–24] and the recent experimental findings [25–29].

In (1), the  $\Delta_J$  measures the depletion of the Fermi sphere at zero momentum with respect to the FFG model while  $\beta_J$  is the strength of the momentum dependence  $I(\mathbf{k}/k_F^J)$  of the depletion near the Fermi surface. Owing to the small effects of  $\beta_J$  on the energy per nucleon [39], we assume  $\beta_J = 0$  in this work. The sketch of  $n_{\mathbf{k}}^J(\rho, \delta)$  is shown in Fig. 1. The isospin structure of the parameters  $\Delta_J$ ,  $C_J$  and  $\phi_J$  is found to be  $Y_J = Y_0(1 + Y_1 \tau_3^J \delta)$  [39]. The amplitude  $C_J$  and high-momentum cutoff coefficient

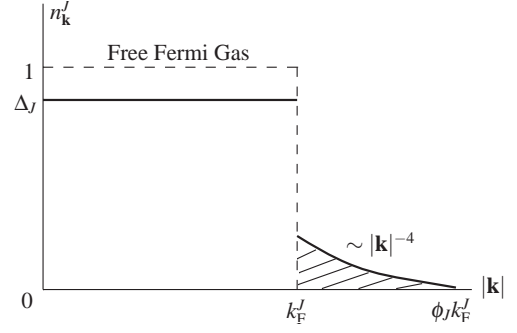


FIG. 1: A sketch of the single-nucleon momentum distribution with a high momentum tail used in this work. Taken from ref. [39].

$\phi_J$  determine the fraction of nucleons in the HMT via

$$x_J^{\text{HMT}} = 3C_J (1 - \phi_J^{-1}). \quad (2)$$

The normalization condition  $[2/(2\pi)^3] \int_0^\infty n_{\mathbf{k}}^J(\rho, \delta) d\mathbf{k} = \rho_J = (k_F^J)^3/3\pi^2$  requires that only two of the three parameters, i.e.,  $C_J$ ,  $\phi_J$  and  $\Delta_J$ , are independent. Here we choose the first two as independent and determine the  $\Delta_J$  by

$$\Delta_J = 1 - 3C_J(1 - \phi_J^{-1}). \quad (3)$$

The  $C/|\mathbf{k}|^4$  shape of the HMT both for SNM and pure neutron matter (PNM) is strongly supported by several recent studies both theoretically and experimentally. Combining the results from analyzing cross sections of  $d(e, e'p)$  reactions [28] and medium-energy photonuclear absorptions [25], the  $C_0$  was found to be  $C_0 \approx 0.161 \pm 0.015$ . With this  $C_0$  and the value of  $x_{\text{SNM}}^{\text{HMT}} = 28\% \pm 4\%$  [27, 28, 38] obtained from systematic analyses of inclusive  $(e, e')$  reactions and data from exclusive two-nucleon knockout reactions, the HMT cutoff parameter in SNM is determined to be  $\phi_0 = (1 - x_{\text{SNM}}^{\text{HMT}}/3C_0)^{-1} = 2.38 \pm 0.56$  [39]. The value of  $C_n^{\text{PNM}} = C_0(1 + C_1)$  was extracted by applying the adiabatic sweep theorem [51] to the EOS of PNM constrained by predictions of microscopic nuclear many-body theories [46–50] and the EOS of cold atoms under unitary condition [51, 52]. More specifically,  $C_n^{\text{PNM}} \approx 0.12$  and  $C_1 = -0.25 \pm 0.07$  were obtained [39]. By inserting the values of  $x_{\text{PNM}}^{\text{HMT}} = 1.5\% \pm 0.5\%$  [27, 28, 38] extracted in the same way as the  $x_{\text{SNM}}^{\text{HMT}}$  and  $C_n^{\text{PNM}}$  into Eq. (2), the high momentum cutoff parameter for PNM was determined to be  $\phi_n^{\text{PNM}} \equiv \phi_0(1 + \phi_1) = (1 - x_{\text{PNM}}^{\text{HMT}}/3C_n^{\text{PNM}})^{-1} = 1.04 \pm 0.02$  [39]. Consequently,  $\phi_1 = -0.56 \pm 0.10$  [39] was obtained by using the  $\phi_0$  determined earlier.

### B. Basic Equations in the Nonlinear Relativistic Mean Field Model Incorporating the SRC-Modified Single Nucleon Momentum Distribution

The nonlinear RMF model has been very successful in describing many nuclear phenomena, see, e.g., refs. [53–

57]. In the following, we outline major ingredients of the nonlinear RMF model we use in this work. The emphasis is on describing where and how the SRC-modified nucleon momentum distribution is used to replace the FFG step function traditionally used in all RMF models.

The interacting Lagrangian of the nonlinear RMF model supplemented with couplings between the isoscalar and the isovector mesons reads [58–67]

$$\begin{aligned}\mathcal{L} = & \bar{\psi} [\gamma_\mu (i\partial^\mu - g_\omega \omega^\mu - g_\rho \vec{\rho}^\mu \cdot \vec{\tau}) - (M - g_\sigma \sigma)] \psi \\ & - \frac{1}{2} m_\sigma^2 \sigma^2 + \frac{1}{2} \partial_\mu \sigma \partial^\mu \sigma - U(\sigma) \\ & + \frac{1}{2} m_\omega^2 \omega_\mu \omega^\mu - \frac{1}{4} \omega_{\mu\nu} \omega^{\mu\nu} + \frac{1}{4} c_\omega (g_\omega \omega_\mu \omega^\mu)^2 \\ & + \frac{1}{2} m_\rho^2 \vec{\rho}_\mu \cdot \vec{\rho}^\mu - \frac{1}{4} \vec{\rho}_{\mu\nu} \cdot \vec{\rho}^{\mu\nu} \\ & + \frac{1}{2} g_\rho^2 \vec{\rho}_\mu \cdot \vec{\rho}^\mu \Lambda_V g_\omega^2 \omega_\mu \omega^\mu,\end{aligned}\quad (4)$$

where  $\omega_{\mu\nu} \equiv \partial_\mu \omega_\nu - \partial_\nu \omega_\mu$  and  $\vec{\rho}_{\mu\nu} \equiv \partial_\mu \vec{\rho}_\nu - \partial_\nu \vec{\rho}_\mu$  are strength tensors for  $\omega$  field and  $\rho$  field, respectively.  $\psi$ ,  $\sigma$ ,  $\omega_\mu$ ,  $\vec{\rho}_\mu$  are nucleon field, isoscalar-scalar field, isoscalar-vector field and isovector-vector field, respectively, and the arrows denote the vector in isospin space,  $U(\sigma) = b_\sigma M (g_\sigma \sigma)^3 / 3 + c_\sigma (g_\sigma \sigma)^4 / 4$  is the self interaction term for  $\sigma$  field.  $\Lambda_V$  represents the coupling constant between the isovector  $\rho$  meson and the isoscalar  $\omega$  meson. In addition,  $M = 939$  MeV is the nucleon mass and  $m_\sigma$ ,  $m_\omega$ ,  $m_\rho$  are masses of mesons.

In the mean field approximation, after neglecting effects of fluctuation and correlation, meson fields are replaced by their expectation values, i.e.,  $\bar{\sigma} \rightarrow \sigma$ ,  $\bar{\omega}_0 \rightarrow \omega_\mu$ ,  $\bar{\rho}_0^{(3)} \rightarrow \vec{\rho}_\mu$ , where subscript “0” indicates zeroth component of the four-vector, superscript “(3)” indicates third component of the isospin. Furthermore, we also use in this work the non-sea approximation which neglects the effect due to negative energy states in the Dirac sea. The mean field equations are then expressed as

$$m_\sigma^2 \bar{\sigma} = g_\sigma [\rho_S - b_\sigma M (g_\sigma \bar{\sigma})^2 - c_\sigma (g_\sigma \bar{\sigma})^3], \quad (5)$$

$$m_\omega^2 \bar{\omega}_0 = g_\omega [\rho - c_\omega (g_\omega \bar{\omega}_0)^3 - \Lambda_V g_\omega \bar{\omega}_0 (g_\rho \bar{\rho}_0^{(3)})^2], \quad (6)$$

$$m_\rho^2 \bar{\rho}_0^{(3)} = g_\rho [\rho_P - \rho_N - \Lambda_V g_\rho \bar{\rho}_0^{(3)} (g_\omega \bar{\omega}_0)^2], \quad (7)$$

where  $\rho = \langle \bar{\psi} \gamma^0 \psi \rangle = \rho_n + \rho_p$  and  $\rho_S = \langle \bar{\psi} \psi \rangle = \rho_{S,n} + \rho_{S,p}$  are the baryon density and scalar density, respectively, with the latter given by

$$\begin{aligned}\rho_{S,J} &= \frac{2}{(2\pi)^3} \int_0^{k_F^J} n_{\mathbf{k}}^J d\mathbf{k} \frac{M_J^*}{\sqrt{|\mathbf{k}|^2 + M_J^{*2}}} \\ &= \frac{2}{(2\pi)^3} \int_0^{k_F^J} \Delta_J d\mathbf{k} \frac{M_J^*}{\sqrt{|\mathbf{k}|^2 + M_J^{*2}}} \\ &\quad + \frac{2}{(2\pi)^3} \int_{k_F^J}^{\phi_J k_F^J} C_J \left( \frac{k_F^J}{|\mathbf{k}|} \right)^4 d\mathbf{k} \frac{M_J^*}{\sqrt{|\mathbf{k}|^2 + M_J^{*2}}}.\end{aligned}\quad (8)$$

The change introduced by the SRC-modified nucleon momentum distribution is in the following replacement

$$\int_0^{k_F^J} (\text{FFG step function}) f d\mathbf{k} \longrightarrow \int_0^{\phi_J k_F^J} n_{\mathbf{k}}^J (\text{HMT}) f d\mathbf{k} \quad (9)$$

with  $f$  being any quantity. In the following, we often use the “HMT model” in this work as the abbreviation for the nonlinear RMF model using the SRC-modified nucleon momentum distribution, while the “FFG model” refers to the original nonlinear RMF model using the FFG step function for the single-nucleon momentum distribution. The Fermi energy of nucleon  $J$  is  $E_F^{J*} = (k_F^{J,2} + M_J^{*,2})^{1/2}$  where  $M_J^*$  is the nucleon Dirac mass defined as

$$M_J^* \equiv M - g_\sigma \bar{\sigma}. \quad (10)$$

The energy-momentum density tensor for the interacting Lagrangian density in Eq. (4) can be written as

$$\begin{aligned}\mathcal{T}^{\mu\nu} = & \bar{\psi} i \gamma^\mu \partial^\nu \psi + \partial^\mu \sigma \partial^\nu \sigma \\ & - \omega^{\mu\eta} \partial^\nu \omega_\eta - \vec{\rho}^{\mu\eta} \partial^\nu \vec{\rho}_\eta - \mathcal{L} g^{\mu\nu},\end{aligned}\quad (11)$$

where  $g_{\mu\nu} = (+, -, -, -)$  is the Minkowski metric. In the mean field approximation, the mean value of time (zero) component of the energy-momentum density tensor is the energy density of the nuclear matter system, i.e.,

$$\begin{aligned}\varepsilon = & \langle \mathcal{T}^{00} \rangle \\ = & \varepsilon_n^{\text{kin}} + \varepsilon_p^{\text{kin}} + \frac{1}{2} \left[ m_\sigma^2 \bar{\sigma}^2 + m_\omega^2 \bar{\omega}_0^2 + m_\rho^2 (\bar{\rho}_0^{(3)})^2 \right] \\ & + \frac{1}{3} b_\sigma (g_\sigma \bar{\sigma})^3 + \frac{1}{4} c_\sigma (g_\sigma \bar{\sigma})^4 + \frac{3}{4} c_\omega (g_\omega \bar{\omega}_0)^4 \\ & + \frac{3}{2} (g_\rho \bar{\rho}_0^{(3)})^2 \Lambda_V (g_\omega \bar{\omega}_0)^2,\end{aligned}\quad (12)$$

where

$$\begin{aligned}\varepsilon_J^{\text{kin}} = & \frac{2}{(2\pi)^3} \int_0^{k_F^J} \Delta_J d\mathbf{k} \sqrt{|\mathbf{k}|^2 + M_J^{*2}} \\ & + \frac{2}{(2\pi)^3} \int_{k_F^J}^{\phi_J k_F^J} C_J \left( \frac{k_F^J}{|\mathbf{k}|} \right)^4 d\mathbf{k} \sqrt{|\mathbf{k}|^2 + M_J^{*2}}\end{aligned}\quad (13)$$

is the kinetic part of the energy density. Similarly, the mean value of space components of the energy-momentum density tensor corresponds to the pressure of the system, i.e.,

$$\begin{aligned}P = & \frac{1}{3} \sum_{j=1}^3 \langle \mathcal{T}^{jj} \rangle \\ = & P_{\text{kin}}^n + P_{\text{kin}}^p - \frac{1}{2} \left[ m_\sigma^2 \bar{\sigma}^2 - m_\omega^2 \bar{\omega}_0^2 - m_\rho^2 (\bar{\rho}_0^{(3)})^2 \right] \\ & - \frac{1}{3} b_\sigma (g_\sigma \bar{\sigma})^3 - \frac{1}{4} c_\sigma (g_\sigma \bar{\sigma})^4 + \frac{1}{4} c_\omega (g_\omega \bar{\omega}_0)^4 \\ & + \frac{1}{2} (g_\rho \bar{\rho}_0^{(3)})^2 \Lambda_V (g_\omega \bar{\omega}_0)^2,\end{aligned}\quad (14)$$



where the kinetic part of pressure is given by

$$P_{\text{kin}}^J = \frac{1}{3\pi^2} \int_0^{k_F^J} \Delta_J dk \frac{k^4}{\sqrt{k^2 + M_J^{*2}}} + \frac{1}{3\pi^2} \int_{k_F^J}^{\phi_J k_F^J} C_J \left( \frac{k_F^J}{k} \right)^4 dk \frac{k^4}{\sqrt{k^2 + M_J^{*2}}}. \quad (15)$$

For completeness, in the following we recall the definitions of several physics quantities characterizing the EOS of SNM and the density dependence of nuclear symmetry energy around  $\rho_0$ . Expressions of these quantities in the presence of the HMT are given in the appendixes. These expressions can be used readily to fix the RMF model parameters by reproducing the empirical values of these quantities at  $\rho_0$ . First of all, the EOS of ANM can be calculated through the energy density  $\varepsilon(\rho, \delta)$  by

$$E(\rho, \delta) = \frac{\varepsilon(\rho, \delta)}{\rho} - M. \quad (16)$$

One important relation holds between the pressure and the energy density,

$$P = \rho^2 \frac{\partial(\varepsilon(\rho, \delta)/\rho)}{\partial \rho}, \quad (17)$$

and in Appendix C, we will prove this relation in SNM.

The function  $E(\rho, \delta)$  can be expanded as a power series of even-order terms in  $\delta$  as

$$E(\rho, \delta) \simeq E_0(\rho) + E_{\text{sym}}(\rho)\delta^2 + \mathcal{O}(\delta^4), \quad (18)$$

where  $E_0(\rho) = E(\rho, \delta = 0)$  is the EOS of SNM, and the symmetry energy is expressed as

$$E_{\text{sym}}(\rho) = \frac{1}{2} \frac{\partial^2 E(\rho, \delta)}{\partial \delta^2} \Big|_{\delta=0}. \quad (19)$$

Around the saturation density  $\rho_0$ , the  $E_0(\rho)$  can be expanded, e.g., up to 2nd-order in density, as,

$$E_0(\rho) = E_0(\rho_0) + \frac{1}{2} K_0 \chi^2 + \mathcal{O}(\chi^3), \quad (20)$$

where  $\chi = (\rho - \rho_0)/3\rho_0$  is a dimensionless variable characterizing the deviations of the density from the saturation density  $\rho_0$ . The first term  $E_0(\rho_0)$  on the right-hand-side

of Eq. (20) is the binding energy per nucleon in SNM at  $\rho_0$  and,

$$K_0 = 9\rho_0^2 \frac{d^2 E_0(\rho)}{d\rho^2} \Big|_{\rho=\rho_0} \quad (21)$$

is the incompressibility coefficient of SNM. Similarly, one can expand the  $E_{\text{sym}}(\rho)$  around the normal density as

$$E_{\text{sym}}(\rho) = E_{\text{sym}}(\rho_0) + L\chi + \mathcal{O}(\chi^2), \quad (22)$$

with the slope parameter  $L$  of the symmetry energy defined by

$$L \equiv 3\rho_0 \frac{dE_{\text{sym}}(\rho)}{d\rho} \Big|_{\rho=\rho_0}. \quad (23)$$

It is necessary to point out here an inconsistency of our approach. Since the phenomenological  $n_{\mathbf{k}}^J$  in Eq. (1) has no direct relation to the interacting Lagrangian (4), although it is constrained by recent experimental and microscopic theoretical studies, our results may have some deviations from those using the  $n_{\mathbf{k}}^J$  obtained in models going beyond the mean field approximation by solving the equation of  $\psi$  in the presence of interactions between nucleons and mesons expressed in the Lagrangian (4) self-consistently. In fact, this inconsistency exists in almost all phenomenological mean-field models. Ideally, one should first reproduce quantitatively the experimentally constrained  $n_{\mathbf{k}}^J$  by adjusting parameters in the model Lagrangian. Unfortunately, as shown by the strong model dependence in predicting the  $n_{\mathbf{k}}^J$  using various models and interactions, our poor knowledge on the isospin dependence of short-range nucleon-nucleon interactions, such as the couplings  $g_\rho$  and  $\Lambda_V$  in (4), still hinders reproducing quantitatively the experimentally constrained  $n_{\mathbf{k}}^J$ . Thus, our hybrid approach using directly the phenomenological  $n_{\mathbf{k}}^J$  constrained by experiments can give us some useful perspectives on the effects of the HMT on the EOS of ANM.

### III. THE KINETIC SYMMETRY ENERGY WITH HIGH MOMENTUM NUCLEONS

As shown in detail in Appendix A, the kinetic symmetry energy  $E_{\text{sym}}^{\text{kin}}(\rho)$  in the RMF model with the HMT can be written as

$$\begin{aligned}
E_{\text{sym}}^{\text{kin}}(\text{HMT}) = & \frac{k_F^2}{6E_F^*} \left[ 1 - 3C_0 \left( 1 - \frac{1}{\phi_0} \right) \right] - 3E_F^* C_0 \left[ C_1 \left( 1 - \frac{1}{\phi_0} \right) + \frac{\phi_1}{\phi_0} \right] \\
& - \frac{9M_0^{*,4}}{8k_F^3} \frac{C_0 \phi_1 (C_1 - \phi_1)}{\phi_0} \left[ \frac{2k_F}{M_0^*} \left( \left( \frac{k_F}{M_0^*} \right)^2 + 1 \right)^{3/2} - \frac{k_F}{M_0^*} \left( \left( \frac{k_F}{M_0^*} \right)^2 + 1 \right)^{1/2} - \text{arcsinh} \left( \frac{k_F}{M_0^*} \right) \right] \\
& + \frac{2k_F C_0 (6C_1 + 1)}{3} \left[ \text{arcsinh} \left( \frac{\phi_0 k_F}{M_0^*} \right) - \sqrt{1 + \left( \frac{M_0^*}{\phi_0 k_F} \right)^2} - \text{arcsinh} \left( \frac{k_F}{M_0^*} \right) + \sqrt{1 + \left( \frac{M_0^*}{k_F} \right)^2} \right] \\
& + \frac{3k_F C_0}{2} \left[ \frac{(1 + 3\phi_1)^2}{9} \left( \frac{\phi_0 k_F}{F_F^*} - \frac{2F_F^*}{\phi_0 k_F} \right) + \frac{2F_F^* (3\phi_1 - 1)}{9\phi_0 k_F} - \frac{1}{9} \frac{k_F}{E_F^*} + \frac{4E_F^*}{9k_F} \right] \\
& + \frac{C_0 (4 + 3C_1)}{3} \left[ \frac{F_F^* (1 + 3\phi_1)}{\phi_0} - E_F^* \right], \tag{24}
\end{aligned}$$

where

$$E_F^* = (M_0^{*,2} + k_F^2)^{1/2} \text{ and } F_F^* = (M_0^{*,2} + (\phi_0 k_F)^2)^{1/2}. \tag{25}$$

In the FFG limit,  $\phi_0 = 1, \phi_1 = 0$ , only the first term of the above expression survives and leads to  $E_{\text{sym}}^{\text{kin}}(\rho) \rightarrow E_{\text{sym}}^{\text{kin}}(\text{FFG}) \equiv k_F^2/6E_F^*$  as in traditional RMF models. The kinetic symmetry energy in the presence of HMT is a function only of the Dirac effective mass  $M_0^*$ . Using the values of  $C_0, C_1, \phi_0$  and  $\phi_1$  given in the last section, we show in Fig. 2 the kinetic symmetry energy as a function of  $M_0^*$  at  $\rho_0 = 0.16 \text{ fm}^{-3}$  for both the FFG and HMT models. In the whole range of  $M_0^*$  considered as reasonable, the kinetic symmetry energy at  $\rho_0$  in the HMT model is always negative. For example, with

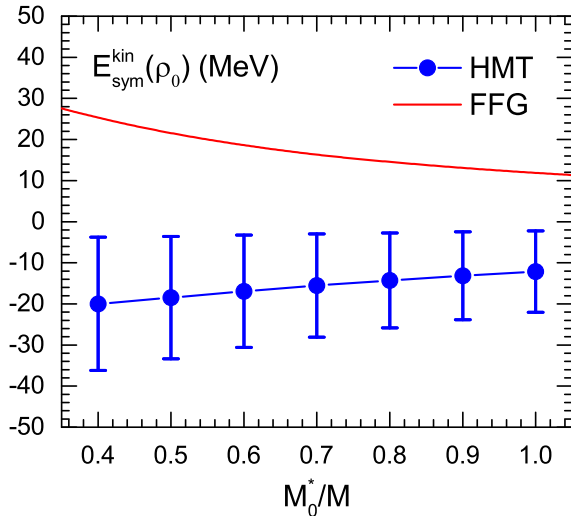


FIG. 2: (Color Online) The kinetic symmetry energy as a function of Dirac effective mass of nucleon in SNM both in the FFG model and in the HMT model,  $\rho_0 = 0.16 \text{ fm}^{-3}$ .

$M_0^*/M = 0.6$  the kinetic symmetry energy is

$$E_{\text{sym}}^{\text{kin}}(\rho_0) = -16.94 \pm 13.66 \text{ MeV} \tag{26}$$

where the errors are all from the uncertainties of  $C_0, C_1, \phi_0$  and  $\phi_1$ . This value is close to the non-relativistic result of  $E_{\text{sym}}^{\text{kin}}(\rho_0) = -13.90 \pm 11.54 \text{ MeV}$  according to the expression [39]

$$\begin{aligned}
E_{\text{sym}}^{\text{kin}}(\rho) = & k_F^2/6M \cdot [1 + C_0(1 + 3C_1)(5\phi_0 + 3/\phi_0 - 8) \\
& + 3C_0\phi_1(1 + 3C_1/5)(5\phi_0 - 3/\phi_0) + 27C_0\phi_1^2/5\phi_0]. \tag{27}
\end{aligned}$$

Thus, the reduction of the kinetic symmetry energy in the presence of HMT is general in both relativistic and non-relativistic calculations [38, 39]. Moreover, this result is also consistent with the findings of several recent studies of the kinetic EOS considering the SRC using both phenomenological models and microscopic many-body theories [31–37].

#### IV. VALIDATION OF SRC-MODIFIED SINGLE-NUCLEON MOMENTUM DISTRIBUTION AND ITS EFFECTS ON THE EOS OF SYMMETRIC NUCLEAR MATTER

First of all, it is necessary to point out that since we fixed the parameters of the nucleon momentum distribution by using experimental data and/or model calculations at the saturation density, the possible density dependence of those parameters, i.e.,  $C_0, C_1, \phi_0$  and  $\phi_1$  is not explored in this work as well as in ref. [39]. The density dependence of the various terms in the kinetic EOS is thus only due to that of the meson fields and the Fermi momenta. In this section, all analytical expressions are obtained under this assumption. The numerical results are obtained by setting  $\phi_0 = 2.38, \phi_1 = -0.56, C_0 = 0.161$  and  $C_1 = -0.25$ . In both the HMT and FFG models, the masses of meson fields are chosen as  $m_\sigma = 500 \text{ MeV}$ ,  $m_\omega = 782.5 \text{ MeV}$ , and  $m_\rho = 763 \text{ MeV}$ .

To determine the EOS and total symmetry energy with the SRC-modified single-nucleon momentum distribution, we need to readjust the RMF model parameters to reproduce all known empirical properties of SNM and

Table I: Coupling constants used in the two RMF models (right side) and some empirical properties of asymmetric nucleonic matter used to fix them (left side).

Quantity	this work	Coupling	FFG	HMT
$\rho_0$ (fm $^{-3}$ )	0.15	$g_\sigma$	10.9310	10.8626
$E_0(\rho_0)$ (MeV)	-16.0	$g_\omega$	14.5947	12.9185
$M_0^*/M$	0.6	$b_\sigma$	0.0007473	0.002119
$K_0$ (MeV)	230.0	$c_\sigma$	0.003882	-0.0005139
$E_{\text{sym}}(\rho_0)$ (MeV)	31.6	$g_\rho$	5.9163	7.8712
$L$ (MeV)	58.9	$\Lambda_V$	0.2736	0.03740

ANM. Thus, analytical expressions for quantities characterizing these properties are necessary. Combining the results derived in detail in the Appendixes, we have expressions for four such quantities for SNM, i.e., the Dirac effective mass  $M_0^*$ ; the binding energy of SNM obtained through  $E_0(\rho) = \varepsilon_0(\rho)/\rho - M$  with  $\varepsilon_0$  given by (C3) together with (C8) and (C10); the pressure  $P_0$  of SNM (C25) and the incompressibility coefficient  $K_0$  of SNM (C30). For ANM, we also need expressions for the total symmetry energy  $E_{\text{sym}}(\rho)$  and its slope  $L$ . While the kinetic symmetry energy  $E_{\text{sym}}^{\text{kin}}(\rho)$  is already given by (24), the potential symmetry energy  $E_{\text{sym}}^{\text{pot}}(\rho)$  can be written as [66, 67]

$$E_{\text{sym}}^{\text{pot}}(\rho) = \frac{g_\rho^2 \rho}{2Q_\rho} \text{ with } Q_\rho = m_\rho^2 + \Lambda_V g_\rho^2 g_\omega^2 \bar{\omega}_0^2. \quad (28)$$

Correspondingly, the slope parameter  $L$  of the total symmetry energy also has two parts, i.e., (B15) with the kinetic part  $L^{\text{kin}}$  given by (B11) and the potential part  $L^{\text{pot}}$  by (B13). The total number of the analytical expressions is now six while there are seven coupling constants in the Lagrangian density (4). We are thus still free to choose one of the seven coupling constants, and in this work we fix the value of  $c_\omega = 0.01$  which is the same as that in the FSUGold parametrization [65]. In this way, given the values of  $M_0^*$ ,  $E_0(\rho_0)$ ,  $\rho_0$ ,  $K_0$ ,  $E_{\text{sym}}(\rho_0)$  and  $L$ , we can uniquely determine the other six coupling constants. Listed in Table I are the coupling constants in both the FFG and HMT models obtained from reproducing the same values of the listed empirical properties of ANM. The value of  $K_0 = 230 \pm 20$  MeV was determined from analyzing nuclear giant resonances (GMR) [68–72]. For the  $E_{\text{sym}}(\rho_0)$  and  $L$ , all existing constraints extracted so far from both terrestrial laboratory measurements and astrophysical observations are found to be essentially consistent with the 2013 global averages of  $E_{\text{sym}}(\rho_0) = 31.6 \pm 2.66$  MeV and  $L = 58.9 \pm 16$  MeV [40]. We notice that the values of the two isovector parameters  $g_\rho$  and  $\Lambda_V$  are significantly different in the HMT and FFG models.

To evaluate the HMT and FFG models, we show in the left panel of Fig. 3 the binding energy and pressure of SNM as functions of density. It is interesting to see that the HMT model predicts a harder EOS for

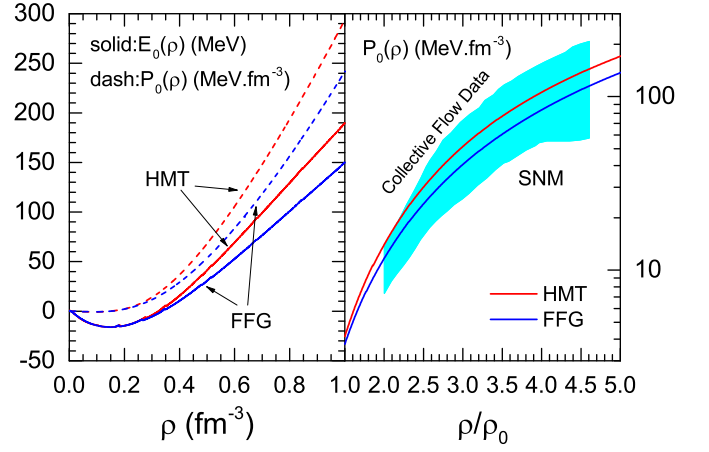


FIG. 3: (Color Online) Left panel: The EOS and pressure  $P_0$  of SNM as functions of density for both the FFG and HMT models; Right panel: a comparison between the model pressure  $P_0$  of SNM with the experimental constraints from analyzing nuclear collective flows in heavy ion collisions.

SNM at supra-saturation densities than the FFG model while by design they both have the same values of  $M_0^*$ ,  $\rho_0$ ,  $E_0(\rho_0)$  and  $K_0$ . This is simply because of the large contribution to the kinetic EOS by the high momentum nucleons in the HMT model. Therefore, the HMT is expected to affect the high order characteristic coefficients of the SNM at  $\rho_0$  compared to calculations with the FFG. More quantitatively, the third-order Taylor expansion coefficient of the EOS of SNM around  $\rho_0$ , i.e., the skewness of the SNM  $Q_0 \equiv 27\rho_0^3 \partial^3 E_0(\rho)/\partial \rho^3|_{\rho=\rho_0}$  [73–75] is changed from  $Q_0^{\text{FFG}} \approx -454$  MeV in the FFG model to  $Q_0^{\text{HMT}} \approx -266$  MeV in the HMT model. Unfortunately, our current knowledge on the parameter  $Q_0$  [74–80] is still too poor to put a constraint on it. On the other hand, the pressure of SNM in the density range of about  $2\rho_0$  to  $5\rho_0$  has been experimentally constrained by measuring nuclear collective flows in heavy-ion collisions [3], which is shown as a cyan band in the right panel of Fig. 3. Although the HMT makes skewness of the SNM higher, it is seen that the pressure of SNM in the presence of HMT can still pass through the constraints from the collective flow data. Namely, the uncertainty band of the constraints on the EOS at supra-saturation densities is too broad to distinguish the HMT and FFG predictions. Thus, as we shall discuss next, additional experimental constraints are necessary to distinguish the two models.

In the nonlinear RMF model, the kinetic EOS of SNM is defined as

$$E_0^{\text{kin}}(\rho) \equiv \frac{1}{\rho} \frac{2}{(2\pi)^3} \int_0^{\phi_0 k_F} n_{\mathbf{k}}^0 \sqrt{\mathbf{k}^2 + M_0^{*2}} d\mathbf{k} - M_0^*, \quad (29)$$

where  $n_{\mathbf{k}}^0$  is the momentum distribution of nucleons in SNM. The HMT and FFG model predictions for the  $E_0^{\text{kin}}(\rho)$  are shown in Fig. 4. Recently, the average kinetic energy of neutrons and protons in C, Al, Fe and Pb with error bars as well as  $^7,8,9\text{Li}$ ,  $^9,10\text{Be}$  and  $^{11}\text{B}$  without error

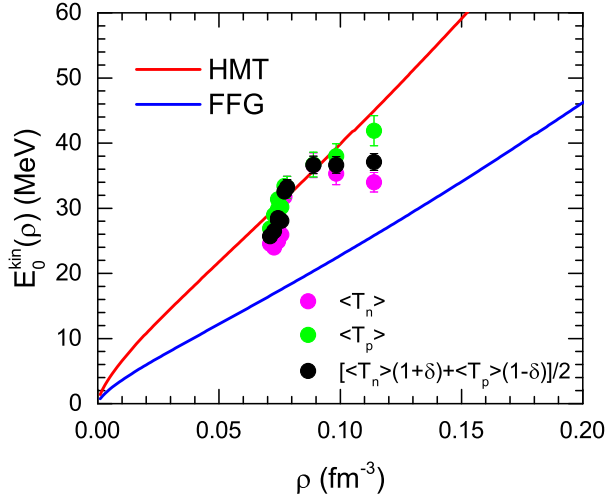


FIG. 4: (Color Online) The kinetic EOS of SNM defined by (29). The experimental kinetic energy of neutrons and protons in C, Al, Fe and Pb with error bars [27] and  ${}^7,8,9\text{Li}$ ,  ${}^9,10\text{Be}$  and  ${}^{11}\text{B}$  [81] were extracted using the neutron-proton dominance model.

bars were extracted from several electron-nucleus scattering experiments using a neutron-proton dominance model [27, 81]. We can translate the  $A$ -dependence of the nucleon kinetic energy into its density dependence through a well-established empirical relationship [82–88]

$$\rho_A \simeq \frac{\rho_0}{1 + \alpha/A^{1/3}} \quad (30)$$

where  $\alpha$  reflects the balance between the volume and surface symmetry energies and in our calculation we adopt  $\alpha = 2.8$  [86] appropriate for the mass range considered. The black points represent the average kinetic energy per nucleon for these nuclei, i.e.,  $\langle T \rangle = [\langle T_n \rangle(1+\delta) + \langle T_p \rangle(1-\delta)]/2$ . According to the parabolic approximation for the EOS of ANM, i.e.,  $E_{\text{ANM}}^{\text{kin}}(\rho) \simeq E_0^{\text{kin}}(\rho) + \delta^2 E_{\text{sym}}^{\text{kin}}(\rho)$ , even for the most neutron-rich nucleus considered  ${}^{208}\text{Pb}$  with an isospin asymmetry  $\delta^2 \simeq 0.045$ , we still have  $E_{\text{ANM}}^{\text{kin}}(\rho) \simeq E_0^{\text{kin}}(\rho)$ . This means that the data in Fig. 4 are approximately equal to the kinetic EOS of SNM  $E_0^{\text{kin}}(\rho)$ . It is very interesting to see that the HMT prediction can well reproduce while the FFG prediction falls about 40% below the data around  $\rho_A = 0.1 \text{ fm}^{-3}$ . This clearly indicates the importance of the HMT in the SRC-modified single nucleon momentum distribution. It is well known that mean-field models fail to describe the spectroscopic factors extracted from electron scatterings on nuclei from  ${}^7\text{Li}$  to  ${}^{208}\text{Pb}$  by about 30-40% due to the lack of occupations of energetic orbitals in these models where the short-range correlations are not considered [89]. The observation here that the FFG model under predicts the average nucleon kinetic energy is due to the same reason and it misses the data by about the same magnitude as in describing the spectroscopic factors.

## V. NUCLEON SCALAR DENSITY AND DIRAC EFFECTIVE MASS IN THE RMF MODEL WITH HIGH MOMENTUM NUCLEONS

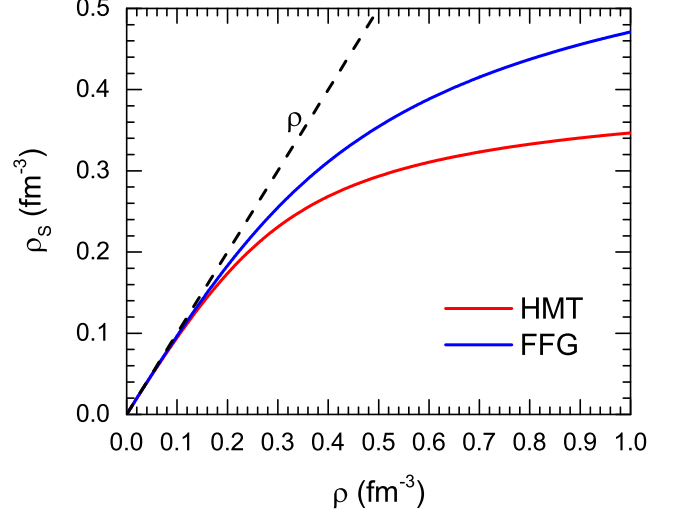


FIG. 5: (Color Online) Scalar density of SNM as a function of baryon density for both the FFG and HMT models.

As discussed earlier, the kinetic symmetry energy depends on the nucleon Dirac effective mass which is determined by the scalar baryon density  $\rho_s$ . It is thus interesting to examine explicitly how the SRC-modified nucleon momentum distribution affects the scalar density and the Dirac effective mass. As shown in Appendix B, see (B12), the scalar density  $\rho_s$  can be written as

$$\rho_s = \frac{\Delta_0 M_0^{*,3}}{\pi^2} \left( \theta \sqrt{1 + \theta^2} - \text{arcsinh} \theta \right) + \frac{2C_0 k_F^4}{\pi^2 M_0^*} \left( \sqrt{1 + \frac{1}{\theta^2}} - \sqrt{1 + \frac{1}{\phi_0^2 \theta^2}} \right) \quad (31)$$

with  $\theta = k_F/M_0^*$ . At low densities, the  $\theta$  is small, thus

$$\theta \sqrt{1 + \theta^2} - \text{arcsinh} \theta \approx \frac{2}{3} \theta^3 - \frac{1}{5} \theta^5, \quad (32)$$

$$\theta^4 \left( \sqrt{1 + \frac{1}{\theta^2}} - \sqrt{1 + \frac{1}{\phi_0^2 \theta^2}} \right) \approx \left( 1 - \frac{1}{\phi_0} \right) \theta^3 + \frac{1}{2} (1 - \phi_0) \theta^5. \quad (33)$$

Keeping only the first term, one has,

$$\begin{aligned} \rho_s &\rightarrow \frac{\Delta_0 M_0^{*,3}}{\pi^2} \frac{2}{3} \theta^3 + \frac{2C_0 M_0^{*,3}}{\pi^2} \left( 1 - \frac{1}{\phi_0} \right) \theta^3 \\ &= \frac{2M_0^{*,3} \theta^3}{3\pi^2} \left[ \Delta_0 + 3C_0 \left( 1 - \frac{1}{\phi_0} \right) \right] = \rho, \end{aligned} \quad (34)$$

and the next order correction to  $\rho_s$  is

$$\frac{M_0^{*,3} \theta^5}{\pi^2} \left[ -\frac{1}{5} + C_0 \left( \frac{8}{5} - \frac{3}{5\phi_0} - \phi_0 \right) \right] \quad (35)$$



which is negative, leading to  $\rho_S < \rho$ . For the FFG model ( $\phi_0 = 1, \phi_1 = 0$ ), the value in the bracket of the above expression is  $-1/5$  while the term  $C_0(8/5 - 3/5\phi_0 - \phi_0)$  is always negative. At the high density limit  $\rho \rightarrow \infty$ , the  $\sigma$  field will saturate at the value of  $\bar{\sigma}^\infty \equiv \bar{\sigma}(\rho = \infty) = M/g_\sigma$  (for the Dirac effective mass  $M_0^* = M - g_\sigma \bar{\sigma}$  approaches zero in this limit). Correspondingly, we obtain  $\rho_S^\infty \equiv \rho_S(\rho = \infty) = M^3[(m_\sigma/g_\sigma M)^2 + b_\sigma + c_\sigma]$  according to Eq. (5). More quantitatively, we have  $\rho_S^\infty(\text{FFG}) \approx 3.29 \text{ fm}^{-3}$  and  $\rho_S^\infty(\text{HMT}) \approx 2.99 \text{ fm}^{-3}$ . Thus, the scalar density in the HMT model is always smaller than that in the FFG model as shown in Fig. 5.

In Fig. 6, the nucleon Dirac effective masses in SNM in the FFG and HMT models are shown. The two models are found to give very similar results. This is easy to understand. On one hand, three points of the effective mass are fixed, i.e.,  $M_0^*(0)/M = 0$ ,  $M_0^*(\rho_0)/M = 0.6$  and  $M_0^*(\infty)/M = 0$ . On the other hand, through Eq. (B9) we know that  $\partial\bar{\sigma}/\partial\rho > 0$ . Thus, the  $M_0^*/M$  monotonically decreases in the whole density range and is concave at large densities. Not surprisingly, meeting all of these common constraints the  $M_0^*(\rho)/M$  in the two models behaves very similarly.

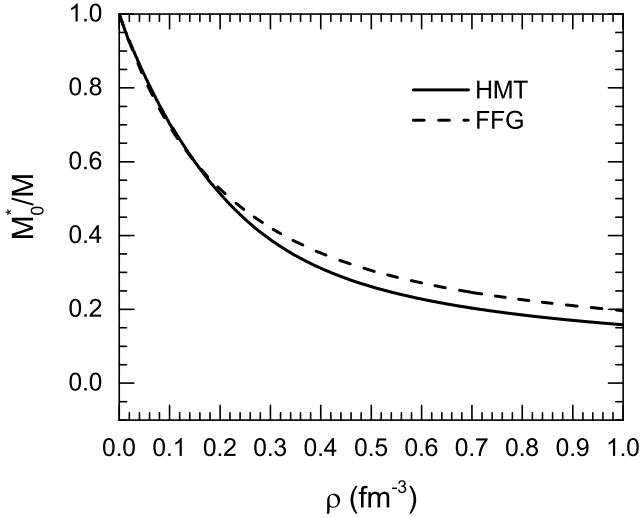


FIG. 6: Nucleon Dirac effective mass in SNM as a function of density for both the FFG and HMT models.

## VI. THE TOTAL SYMMETRY ENERGY IN THE RMF MODEL WITH HIGH MOMENTUM NUCLEONS

We now turn to the total symmetry energy  $E_{\text{sym}}(\rho)$ . Shown in Fig. 7 are the HMT and FFG model predictions in comparison with results from several recent studies by others [8, 88, 90]. It is seen from the upper panel that the HMT softens the  $E_{\text{sym}}(\rho)$  at sub-saturation densities. For instance, at densities around  $0.04 \text{ fm}^{-3}$ , the effect is about 30% which is larger than the width of the existing

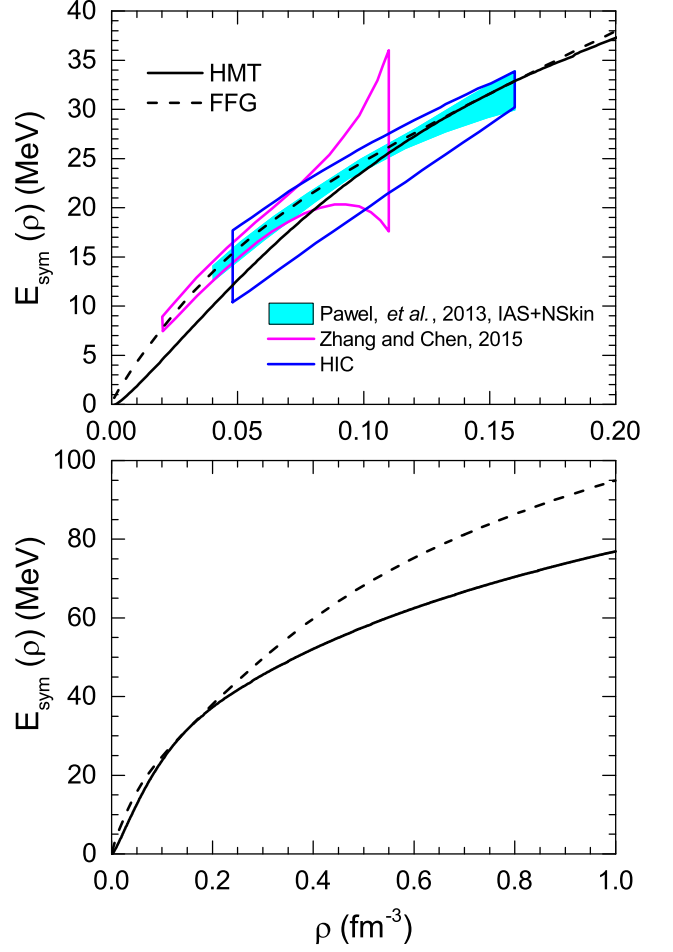


FIG. 7: (Color Online) The total symmetry energy as a function of density in the HMT and FFG models in comparison with constraints from several recent studies [8, 88, 90].

constraint [90]. Interestingly, at supra-saturation densities as shown in the lower panel, the symmetry energy is also significantly softened by the HMT. For instance, the effect is about 25% at densities around  $0.5 \text{ fm}^{-3}$ . Thus, the HMT in the nucleon momentum distribution provides a possible mechanism to soften the symmetry energy at both low and high densities. Actually in the original nonlinear RMF model, the high density  $E_{\text{sym}}(\rho)$  can not be made arbitrary small because of the structure of the model itself. In the presence of HMT, however, mainly owing to the negative kinetic symmetry energy it is possible that the total  $E_{\text{sym}}(\rho)$  becomes very soft and even decreases at high densities as indicated by some data analyses [91].

Since the HMT and FFG models are designed to have the same values of symmetry energy  $E_{\text{sym}}(\rho_0)$  and its slope  $L$ , it is useful to use the curvature of the symmetry

energy

$$K_{\text{sym}} \equiv \left[ 9\rho^2 \frac{\partial^2 E_{\text{sym}}(\rho)}{\partial \rho^2} \right]_{\rho_0} = \left[ 3\rho \frac{\partial L(\rho)}{\partial \rho} - 3L(\rho) \right]_{\rho_0} \quad (36)$$

to measure the HMT effects on the total symmetry energy. The  $K_{\text{sym}}$  is relevant for studying the isospin dependence of the incompressibility of ANM through the relationship

$$K(\delta) \approx K_0 + K_\tau \delta^2 + \mathcal{O}(\delta^4) \quad (37)$$

where the  $K_\tau$  is given by [73]

$$K_\tau = K_{\text{sym}} - 6L - \frac{Q_0 L}{K_0}. \quad (38)$$

More quantitatively, we obtained the values of  $K_{\text{sym}}^{\text{FFG}} \approx -37 \text{ MeV}$  and  $K_{\text{sym}}^{\text{HMT}} \approx -274 \text{ MeV}$ . The corresponding isospin-coefficients of the incompressibility are  $K_\tau^{\text{FFG}} \approx -174 \text{ MeV}$  and  $K_\tau^{\text{HMT}} \approx -470 \text{ MeV}$ . The latter is in very good agreement with the best estimate of  $K_\tau = -550 \pm 100 \text{ MeV}$  from analyzing many different kinds of experimental data currently available [72]. Overall, the HMT is to make the symmetry energy significantly more concave around the saturation density, leading to a stronger isospin dependence in the incompressibility of ANM compared to calculations using the FFG model.

## VII. SOME EFFECTS OF HIGH MOMENTUM NUCLEONS ON PROPERTIES OF NEUTRON STARS

The SRC-modified single-nucleon momentum distribution is expected to affect some properties of neutron stars, see, e.g., ref. [92]. First of all, the softening of the symmetry energy is generally expected to reduce the proton fraction  $x_p = \rho_p/\rho$  in neutron stars within the parabolic approximation of the EOS of ANM. For example, in the npe matter at  $\beta$  equilibrium, according to the chemical equilibrium and charge neutrality conditions for reactions of  $n \rightarrow p + e + \bar{\nu}_e$  and  $p + e \rightarrow n + \nu_e$ , we have  $\mu_e = \mu_n - \mu_p$  where  $\mu_e = [m_e^2 + (k_F^e)^2]^{1/2} = [m_e^2 + (3\pi^2 \rho x_e)^{2/3}]^{1/2} \simeq (3\pi^2 \rho x_e)^{1/3}$  with  $x_e \equiv \rho_e/\rho$  the electron fraction, i.e.,  $\mu_e = \mu_n - \mu_p \approx 4E_{\text{sym}}(\rho)\delta + \mathcal{O}(\delta^3)$ . Thus, the  $x_p = x_e$  will be reduced if the symmetry energy  $E_{\text{sym}}(\rho)$  decreases. However, we caution that although high order terms in the EOS of ANM are relatively small, they still have non-negligible effects on the  $x_p$  in the RMF models [67]. Expectations based on the parabolic approximation for the EOS of ANM may be altered. Moreover, it was suggested recently in ref. [93] that the neutrino emissivity of the direct URCA process will be reduced by a factor  $\eta = Z_F^p Z_F^n$  compared to the FFG model with  $Z_F^J$  the discontinuity of the single-nucleon momentum distribution at the Fermi momentum. In the HMT model, the depletion of the Fermi sphere together with the sizable value of

$C_J$  makes the factor  $\eta$  much smaller than unity. However, effects of nucleons in the HMT not considered in ref. [93] may enhance the emissivity of neutrinos [92, 94]. Thus, to our best knowledge, the net effects of the entire single-nucleon momentum distribution modified by the SRC on both the critical density for the direct URCA process to occur and the cooling rate of protoneutron stars are still unclear. Nevertheless, it is interesting to note that efforts to clarify the issue are currently underway [95].

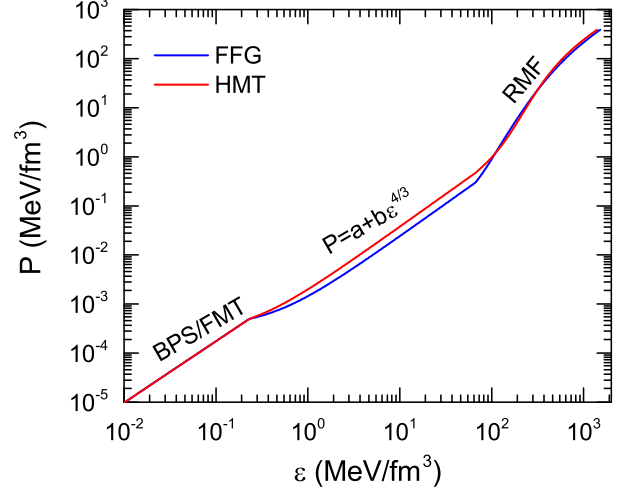


FIG. 8: (Color Online) EOS of neutron star matter. Detailed descriptions of the compositions of different layers of the neutron stars are explained in the text.

Next, we investigate effects of the HMT on the mass-radius relation of neutron stars. In constructing the EOS of various layers in neutron stars for solving the Tolman-Oppenheimer-Volkoff (TOV) equation, we follow a standard scheme. Neutron stars are composed of the npe matter at low densities as described above. For the core we use the EOS of  $\beta$ -stable and charge neutral npe $\mu$  matter obtained from the nonlinear RMF model described earlier. When the chemical potential of electron is larger than the static mass of a muon, reactions  $e \rightarrow \mu + \nu_e + \bar{\nu}_\mu$ ,  $p + \mu \rightarrow n + \nu_\mu$  and  $n \rightarrow p + \mu + \bar{\nu}_\mu$  will also take place. The latter requires

$$\mu_n - \mu_p = \mu_\mu = \sqrt{m_\mu^2 + (3\pi^2 \rho x_\mu)^{2/3}} \quad (39)$$

besides  $\mu_n - \mu_p = \mu_e$ , where  $m_\mu = 105.7 \text{ MeV}$  is the mass of a muon and  $x_\mu \equiv \rho_\mu/\rho$  is the muon fraction. The inner crust with densities ranging between  $\rho_{\text{out}} = 2.46 \times 10^{-4} \text{ fm}^{-3}$  corresponding to the neutron dripline and the core-crust transition density  $\rho_t$  is the region where some complex and exotic structures—collectively referred to as the “nuclear pasta” may exist. Because of our poor knowledge about this region we adopt the polytropic EOSs parameterized in terms of the pressure  $P$  as a function of total energy density  $\varepsilon$  according to  $P = a + b\varepsilon^{4/3}$  [96, 97]. The constants  $a$  and  $b$  are determined by the pressure and energy density at  $\rho_t$  and  $\rho_{\text{out}}$  [96]. For the outer

crust [98], we use the BPS EOS for the region with  $6.93 \times 10^{-13} \text{ fm}^{-3} < \rho < \rho_{\text{out}}$  and the FMT EOS for  $4.73 \times 10^{-15} \text{ fm}^{-3} < \rho < 6.93 \times 10^{-13} \text{ fm}^{-3}$ , respectively.

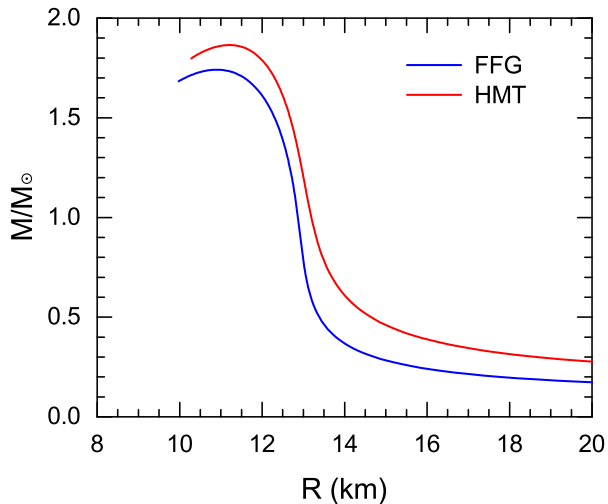


FIG. 9: (Color Online) Mass-radius of a neutron star obtained by integrating the TOV equation under the EOS of neutron star matter in the FFG and HMT models, respectively.

Shown in Fig. 8 are the EOSs of neutron star matter obtained within the FFG and HMT models. The similarity of the two model EOSs indicates that the corresponding mass-radius relations will not be different dramatically. In Fig. 9, the corresponding mass-radius relations of neutron stars from the two model are compared. As discussed earlier in Section IV, the skewness of SNM mainly characterizes the high density behavior of the EOS of SNM. The SRC induced HMT is to increase the skewness of SNM and thus hardens the EOS of neutron star matter. On the other hand, the symmetry energy effect on the mass-radius relation of neutron stars is relatively smaller in the RMF models [99]. Therefore, the enhanced skewness  $Q_0$  due to the HMT enlarges the maximum mass of neutron stars as shown in the Fig. 9. Quantitatively, the maximum mass of neutron stars in the HMT and FFG models are  $M^{\text{max}} \approx 1.87 M_{\odot}$  and  $M^{\text{max}} \approx 1.74 M_{\odot}$ , with the corresponding radii being about 11.21 km and 10.89 km, respectively. The relative effect on the maximum mass is about 8%. While the maximum mass is still below the observational data, the EOS with HMT helps improve the situation.

## VIII. SUMMARY AND REMARKS

In summary, within the nonlinear RMF model incorporating the SRC-modified single-nucleon momentum distribution constrained by findings of recent electron-nucleus scattering experiments, we have studied the EOS of asymmetric nucleonic matter. In particular, the kinetic symmetry energy in the presence of SRC-induced

high momentum nucleons is found to be  $E_{\text{sym}}^{\text{kin}}(\rho_0) = -16.94 \pm 13.66 \text{ MeV}$  consistent with earlier findings in non-relativistic models. Similar to the findings about the nucleon spectroscopic factors, the average nucleon kinetic energy extracted from electron-nucleus scattering experiments can not be reproduced by traditional RMF models lacking correlations. Including the SRC-induced high momentum nucleons in the RMF model, the data can be well reproduced. Comparing the RMF calculations with and without the SRC-induced high momentum nucleons using two sets of model parameters both reproducing identically all empirical properties of SNM and the symmetry energy of ANM at  $\rho_0$ , the SRC-modified single-nucleon momentum distribution is found to make the EOS of SNM much harder at supra-saturation densities and the  $E_{\text{sym}}(\rho)$  more concave around  $\rho_0$ , leading to a larger maximum mass of neutron stars and an isospin-dependent incompressibility of ANM in better agreement with existing observational/experimental data.

After introducing the SRC-induced high momentum nucleons, some isovector parameters of the RMF model had to be readjusted to reproduce the same empirical properties of ANM and known experimental constraints. Ramifications of these changes and the resulting symmetry energy on experimental observables, such as neutron skins of heavy nuclei will be studied in the near future. The SRC and some of its effects in nuclear structures and reactions are well established both theoretically and experimentally. While the RMF model has been very successful in helping us understand many fundamental physics and explaining various experimental phenomena, as a mean-field model by design it lacks correlations that are important and necessary in understanding some other experimental phenomena. Going beyond the mean-field level, we take one step forward by replacing the step function with an experimentally constrained momentum distribution incorporating the SRC-induced HMT in reformulating some aspects of the nonlinear RMF model. Compared with fully microscopic many-body theories where effects of the SRC are considered self consistently, our hybrid approach is relatively simple but transparent and all relevant physical quantities are given analytically. While much more work remains to be done, the analyses and numerical results presented here are instructive for better understanding effects of the SRC on the EOS of neutron-rich nucleonic matter which is relevant for both nuclear physics and astrophysics.

## Acknowledgement

We would like to thank William G. Newton and Isaac Vidaña for helpful discussions. This work was supported in part by the U.S. National Science Foundation under Grant No. PHY-1068022, the U.S. Department of Energy's Office of Science under Award Number DE-SC0013702 and the National Natural Science Foundation of China under grant no. 11320101004.

### Appendix A: The Derivation of $E_{\text{sym}}^{\text{kin}}(\rho)$

In order to use the following elementary formula,

We start from the kinetic energy density of (13)

$$\begin{aligned} \varepsilon_J^{\text{kin}} &= \frac{\Delta_J}{\pi^2} \int_0^{k_J} k^2 \sqrt{k^2 + m_J^2} dk \\ &+ \frac{C_J k_J^4}{\pi^2} \int_{k_J}^{\phi_J k_J} \frac{1}{k^2} \sqrt{k^2 + m_J^2} dk. \end{aligned} \quad (\text{A1})$$

Using the abbreviations of  $m_J \equiv M_J^*$ ,  $k_J = k_F^J$ ,  $\xi = k/m_J$ ,  $p_J = \phi_J k_J$ , the kinetic energy density can be expressed as

$$\begin{aligned} \varepsilon_J^{\text{kin}} &= \frac{\Delta_J m_J^4}{\pi^2} \int_0^{k_J/m_J} \xi^2 \sqrt{1 + \xi^2} d\xi \\ &+ \frac{C_J k_J^4}{\pi^2} \int_{k_J/m_J}^{\phi_J k_J/m_J} \frac{\sqrt{1 + \xi^2}}{\xi^2} d\xi. \end{aligned} \quad (\text{A2})$$

we rewrite the kinetic energy density as

---


$$\varepsilon_J^{\text{kin}} = \frac{\Delta_J m_J^4}{\pi^2} \int_0^{k_J/m_J} \xi^2 \sqrt{1 + \xi^2} d\xi + \frac{C_J k_J^4}{\pi^2} \left[ \int_0^{p_J/m_J} \frac{\sqrt{1 + \xi^2}}{\xi^2} d\xi - \int_0^{k_J/m_J} \frac{\sqrt{1 + \xi^2}}{\xi^2} d\xi \right], \quad (\text{A4})$$

then its derivative with respect to the isospin asymmetry  $\delta$  is

$$\begin{aligned} \varepsilon_J^{\text{kin}'} &= \frac{4m_J' \Delta_J m_J^3 + \Delta_J' m_J^4}{\pi^2} \cdot \int_0^{k_J/m_J} \xi^2 \sqrt{1 + \xi^2} d\xi + \frac{k_J' \Delta_J k_J^2 E_J^*}{\pi^2} - \frac{m_J' \Delta_J k_J^3 E_J^*}{\pi^2 m_J} \\ &+ \frac{4k_J' C_J k_J^3 + C_J' k_J^4}{\pi^2} \cdot \int_{k_J/m_J}^{p_J/m_J} \frac{\sqrt{1 + \xi^2}}{\xi^2} d\xi + \frac{C_J k_J^4}{\pi^2} \cdot \left( \frac{p_J' F_J^*}{p_J^2} - \frac{m_J' F_J^*}{p_J m_J} - \frac{k_J' E_J^*}{k_J^2} + \frac{m_J' E_J^*}{k_J m_J} \right) \end{aligned} \quad (\text{A5})$$

where  $F_J^* = (p_J^2 + m_J^2)^{1/2} = (\phi_J^2 k_J^2 + m_J^2)^{1/2}$ .

The second order derivative of  $\varepsilon_J^{\text{kin}}$  with respect to  $\delta$  can be obtained in a similar way, i.e.,

$$\begin{aligned} \varepsilon_J^{\text{kin}''} &= \frac{1}{\pi^2} (8\Delta_J' m_J' m_J^3 + 12m_J'^2 \Delta_J m_J^2 + 4m_J'' \Delta_J m_J^3 + \Delta_J'' m_J^4) \int_0^{k_J/m_J} \xi^2 \sqrt{1 + \xi^2} d\xi \\ &+ \frac{1}{\pi^2 m_J} (m_J' k_J' \Delta_J k_J^2 E_J^* + \Delta_J' k_J' k_J^2 m_J E_J^* - 2\Delta_J' m_J' k_J^3 E_J^* - m_J' E_J^{*'} \Delta_J k_J^3 - m_J'' E_J^* \Delta_J k_J^3) \\ &+ \frac{1}{\pi^2} (\Delta_J' k_J' k_J^2 E_J^* + 2k_J'^2 \Delta_J k_J E_J^* + k_J' E_J^{*'} \Delta_J k_J^2 + k_J'' \Delta_J k_J^2 E_J^*) - \frac{3m_J'^2 \Delta_J k_J^3 E_J^*}{\pi^2 m_J^2} \\ &+ \frac{1}{\pi^2} (8C_J' k_J' k_J^3 + 12k_J'^2 C_J k_J^2 + 4k_J'' C_J k_J^3 + C_J'' k_J^4) \int_{k_J/m_J}^{p_J/m_J} \frac{\sqrt{1 + \xi^2}}{\xi^2} d\xi \\ &+ \frac{8k_J' C_J k_J^3 + 2C_J' k_J^4}{\pi^2} \cdot \left( \frac{p_J' F_J^*}{p_J^2} - \frac{m_J' F_J^*}{p_J m_J} - \frac{k_J' E_J^*}{k_J^2} + \frac{m_J' E_J^*}{k_J m_J} \right) \\ &+ \frac{C_J k_J^4}{\pi^2} \cdot \left( \frac{F_J^{*'} p_J'}{p_J^2} + \frac{F_J^* p_J'}{p_J^2} - \frac{2F_J^* p_J'^2}{p_J^3} - \frac{F_J^{*'} m_J'}{p_J m_J} - \frac{F_J^* m_J''}{p_J m_J} + \frac{F_J^* m_J' p_J'}{p_J^2 m_J} + \frac{F_J^* m_J'^2}{p_J m_J^2} \right) \\ &- \frac{C_J k_J^4}{\pi^2} \cdot \left( \frac{E_J^{*'} k_J'}{k_J^2} + \frac{E_J^* k_J''}{k_J^2} - \frac{2E_J^* k_J'^2}{k_J^3} - \frac{E_J^{*'} m_J'}{k_J m_J} - \frac{E_J^* m_J''}{k_J m_J} + \frac{E_J^* m_J' k_J'}{k_J^2 m_J} + \frac{E_J^* m_J'^2}{k_J m_J^2} \right). \end{aligned} \quad (\text{A6})$$

We introduce the abbreviations  $f \equiv \bar{\sigma}$ ,  $w \equiv \bar{w}_0$ , and a subscript “0” denotes the symmetric case, for example,  $f_0 \equiv f(\delta = 0)$ ,  $f'_0 = \partial f / \partial \delta|_{\delta=0}$ , etc. The scalar density is a function of  $m_J$ , i.e.,  $\rho_{S,J} = \rho_{S,J}(m_J)$ , then  $\rho'_{S,J} = \lambda_J m_J'$  with  $\lambda_J$  a certain factor. From the field equation of  $f$ , it is easy to find that  $f'_0 = 0$ . This means that we can omit



the terms proportional to  $m'_J$  in the expression of  $\varepsilon_J^{\text{kin}''}$  (since the symmetry energy is obtained by taking  $\delta = 0$  in  $\varepsilon_J^{\text{kin}''}$ ), thus we have (omitting the terms proportional to  $m'_J$ )

$$\begin{aligned}\varepsilon_J^{\text{kin}''} = & \frac{1}{\pi^2} (4m''_J \Delta_J m_J^3 + \Delta_J'' m_J^4) \cdot \int_0^{k_J/m_J} \xi^2 \sqrt{1+\xi^2} d\xi + \frac{1}{\pi^2 m_J} (\Delta'_J k'_J k_J^2 m_J E_J^* - m''_J E_J^* \Delta_J k_J^3) \\ & + \frac{1}{\pi^2} \left( \Delta'_J k'_J k_J^2 E_J^* + 2k_J'^2 \Delta_J k_J E_J^* + k'_J E_J^{*'} \Delta_J k_J^2 + k_J'' \Delta_J k_J^2 E_J^* \right) + \frac{8k'_J C_J k_J^3 + 2C_J' k_J^4}{\pi^2} \cdot \left( \frac{p'_J F_J^*}{p_J^2} - \frac{k'_J E_J^*}{k_J^2} \right) \\ & + \frac{1}{\pi^2} (8C_J' k'_J k_J^3 + 12k_J'^2 C_J k_J^2 + 4k_J'' C_J k_J^3 + C_J'' k_J^4) \int_{k_J/m_J}^{p_J/m_J} \frac{\sqrt{1+\xi^2}}{\xi^2} d\xi \\ & + \frac{C_J k_J^4}{\pi^2} \cdot \left( \frac{F_J^{*'} p'_J}{p_J^2} + \frac{F_J^* p_J''}{p_J^2} - \frac{2F_J^* p_J'^2}{p_J^3} - \frac{F_J^* m_J''}{p_J m_J} \right) - \frac{C_J k_J^4}{\pi^2} \cdot \left( \frac{E_J^{*'} k'_J}{k_J^2} + \frac{E_J^* k_J''}{k_J^2} - \frac{2E_J^* k_J'^2}{k_J^3} - \frac{E_J^* m_J''}{k_J m_J} \right). \quad (\text{A7})\end{aligned}$$

We then deal with the terms proportional to the second derivative of  $m''_J$ , i.e.,

$$\Pi = m''_J \left[ \frac{4}{m_J} \frac{\Delta_J m_J^4}{\pi^2} \int_0^{k_J/m_J} \xi^2 \sqrt{1+\xi^2} d\xi - \frac{\Delta_J k_J^3 E_J^*}{\pi^2 m_J} - \frac{C_J k_J^4}{\pi^2} \left( \frac{F_J^*}{p_J m_J} - \frac{E_J^*}{k_J m_J} \right) \right]. \quad (\text{A8})$$

Moreover,

$$V = \int_0^{k_J/m_J} \xi^2 \sqrt{1+\xi^2} d\xi = \frac{1}{4} x(x^2+1)^{3/2} - \frac{1}{8} x(x^2+1)^{1/2} - \frac{1}{8} \text{arcsinh } x, \quad (\text{A9})$$

$$S = \int_0^{k_J/m_J} \frac{\xi^2 d\xi}{\sqrt{1+\xi^2}} = \frac{1}{2} x(x^2+1)^{1/2} - \frac{1}{2} \text{arcsinh } x, \quad (\text{A10})$$

with  $x = k_J/m_J$ . For  $k < k_J$ , we then have

$$\varepsilon_J^{\text{kin,I}} = \frac{\Delta_J m_J^4}{\pi^2} \int_0^{k_J/m_J} \xi^2 \sqrt{1+\xi^2} d\xi = \frac{\Delta_J m_J^4 V}{\pi^2}, \quad \rho_{\text{S},J}^{\text{I}} = \frac{\Delta_J m_J^3}{\pi^2} \int_0^{k_J/m_J} \frac{\xi^2 d\xi}{\sqrt{1+\xi^2}} = \frac{\Delta_J m_J^3 S}{\pi^2}, \quad (\text{A11})$$

so

$$\varepsilon_J^{\text{kin,I}} = \frac{\Delta_J k_J^3 E_J^*}{4\pi^2} + \frac{m_J}{4} \rho_{\text{S},J}^{\text{I}}. \quad (\text{A12})$$

On the other hand, the high momentum part of the scalar density should be written as

$$\rho_{\text{S},J}^{\text{II}} = \frac{C_J k_J^4}{\pi^2 m_J} \int_{k_J/m_J}^{p_J/m_J} \frac{d\xi}{\xi^2 \sqrt{1+\xi^2}} = -\frac{C_J k_J^4}{\pi^2 m_J} \left( \frac{F_J^*}{p_J} - \frac{E_J^*}{k_J} \right). \quad (\text{A13})$$

Then  $\Pi$  should be rewritten as

$$\Pi = m''_J \left[ \frac{4}{m_J} \left( \frac{\Delta_J k_J^3 E_J^*}{4\pi^2} + \frac{m_J}{4} \rho_{\text{S},J}^{\text{I}} \right) - \frac{\Delta_J k_J^3 E_J^*}{\pi^2 m_J} + \rho_{\text{S},J}^{\text{II}} \right] = \rho_{\text{S},J} m''_J. \quad (\text{A14})$$

After combining this term with the corresponding potential terms in the energy density, it is found that there exist no terms proportional to  $f_0''$  according to the equation of motion of  $f$ , thus it is safe to write  $\varepsilon_J^{\text{kin}''}$  as (omitting the terms proportional to  $m''_J$ )

$$\begin{aligned}\varepsilon_J^{\text{kin}''} = & \frac{\Delta_J'' m_J^4}{\pi^2} \int_0^{k_J/m_J} \xi^2 \sqrt{1+\xi^2} d\xi + \frac{1}{\pi^2} \left( 2\Delta'_J k'_J k_J^2 E_J^* + 2k_J'^2 \Delta_J k_J E_J^* + k'_J E_J^{*'} \Delta_J k_J^2 + k_J'' \Delta_J k_J^2 E_J^* \right) \\ & + \frac{1}{\pi^2} (8C_J' k'_J k_J^3 + 12k_J'^2 C_J k_J^2 + 4k_J'' C_J k_J^3) \cdot \int_{k_J/m_J}^{p_J/m_J} \frac{\sqrt{1+\xi^2}}{\xi^2} d\xi \\ & + \frac{8k'_J C_J k_J^3 + 2C_J' k_J^4}{\pi^2} \cdot \left( \frac{p'_J F_J^*}{p_J^2} - \frac{k'_J E_J^*}{k_J^2} \right) \\ & + \frac{C_J k_J^4}{\pi^2} \cdot \left( \frac{F_J^{*'} p'_J}{p_J^2} + \frac{F_J^* p_J''}{p_J^2} - \frac{2F_J^* p_J'^2}{p_J^3} \right) - \frac{C_J k_J^4}{\pi^2} \cdot \left( \frac{E_J^{*'} k'_J}{k_J^2} + \frac{E_J^* k_J''}{k_J^2} - \frac{2E_J^* k_J'^2}{k_J^3} \right), \quad (\text{A15})\end{aligned}$$

where the terms proportional to  $C_J''$  are also omitted for  $C_J$  is linear in  $\delta$ , i.e.,  $C_J'' = 0$ .

For

$$Y_J = Y_0(1 + Y_1 \tau_3^J \delta) \quad (\text{A16})$$

with  $Y = C, \phi$ , we have

$$Y_J' = Y_0 Y_1 \tau_3^J. \quad (\text{A17})$$

Thus

$$\begin{aligned}\Delta'_J &= -3C'_J \left(1 - \frac{1}{\phi_J}\right) - \frac{3C_J\phi'_J}{\phi_J^2} \\ &\longrightarrow -3C_0 \left[C_1 \left(1 - \frac{1}{\phi_0}\right) + \frac{\phi_1}{\phi_0}\right] \tau_3^J, \quad (\text{A18})\end{aligned}$$

$$\begin{aligned}\Delta''_J &= -\frac{6C'_J\phi'_J}{\phi_J^2} + \frac{6C_J\phi_J'^2}{\phi_J^3} \\ &\longrightarrow -\frac{6C_0\phi_1}{\phi_0} (C_1 - \phi_1), \quad (\text{A19})\end{aligned}$$

and

$$k'_J = \frac{1}{3}k_F\tau_3^J(\alpha\delta + \dots) \longrightarrow \frac{1}{3}k_F\tau_3^J, \quad (\text{A20})$$

$$k''_J = -\frac{2}{9}k_F(\beta\delta + \dots) \longrightarrow -\frac{2}{9}k_F, \quad (\text{A21})$$

$$p'_J = \phi'_J k_J + \phi_J k'_J \longrightarrow \left(\phi_1 + \frac{1}{3}\right) \phi_0 k_F \tau_3^J, \quad (\text{A22})$$

$$p''_J = 2\phi'_J k'_J + \phi_J k''_J \longrightarrow \frac{2}{3}\phi_0 k_F \left(\phi_1 - \frac{1}{3}\right), \quad (\text{A23})$$

$$E_J^* = \frac{m_J m'_J + k_J k'_J}{E_J^*} \longrightarrow \frac{k_F^2}{3E_F^*} \tau_3^J, \quad (\text{A24})$$

$$F_J^* = \frac{m_J m'_J + p_J p'_J}{F_J^*} \longrightarrow \frac{\phi_0^2 k_F^2 (1 + 3\phi_1)}{3F_F^*} \tau_3^J, \quad (\text{A25})$$

where “ $\longrightarrow$ ” means the limit of  $\delta = 0$ . It is clear that in the FFG model,  $\phi_0 = 1, \phi_0 = 1$ , then

$$\Delta_J \longrightarrow 1, \quad \Delta'_J, \Delta''_J \longrightarrow 0, \quad (\text{A26})$$

and

$$\varepsilon_J^{\text{kin}''} = \frac{1}{\pi^2} \left( 2k_J'^2 k_J E_J^* + k_J' E_J^* k_J^2 + k_J'' k_J^2 E_J^* \right),$$

which is expected. Evaluating  $\sum_{J=n,p} \varepsilon_J^{\text{kin}''}|_{\delta=0}$  according to (A15) and then dividing it by  $2\rho$ , we shall obtain (24).

## Appendix B: The Derivation of $L(\rho)$

In order to derive the expressions for  $L$ , we should first obtain an expression for  $\partial f_0 / \partial \rho$ , which is related to the scalar density that can be decomposed into two terms, i.e.,

$$\rho_S = \frac{2\Delta_0}{\pi^2} \int_0^{k_F} \frac{k^2 dk M_0^*}{\sqrt{k^2 + M_0^{*,2}}} + \frac{2C_0 k_F^4}{\pi^2} \int_{k_F}^{p_F} \frac{1}{k^4} \frac{k^2 dk M_0^*}{\sqrt{k^2 + M_0^{*,2}}}, \quad (\text{B1})$$

where  $M_0^* = M - g_\sigma f_0$ . Putting  $k = \zeta M_0^*$ , then

$$\rho_S = \rho_S^I + \rho_S^{II} = \frac{2\Delta_0 M_0^{*,3}}{\pi^2} \int_0^{k_F/M_0^*} \frac{\zeta^2 d\zeta}{\sqrt{1 + \zeta^2}} + \frac{2C_0 k_F^4}{\pi^2 M_0^*} \int_{k_F/M_0^*}^{p_F/M_0^*} \frac{d\zeta}{\zeta^2 \sqrt{1 + \zeta^2}}, \quad (\text{B2})$$

so

$$\begin{aligned}\frac{\partial \rho_S^I}{\partial \rho} &= \frac{6\Delta_0 M_0^{*,2}}{\pi^2} \frac{\partial M_0^*}{\partial \rho} \int_0^{k_F/M_0^*} \frac{\zeta^2 d\zeta}{\sqrt{1 + \zeta^2}} + \frac{2\Delta_0 M_0^{*,3}}{\pi^2} \frac{(k_F/M_0^*)^2}{\sqrt{1 + (k_F/M_0^*)^2}} \frac{\partial}{\partial \rho} \frac{k_F}{M_0^*} \\ &= \frac{3}{M_0^*} \frac{\partial M_0^*}{\partial \rho} \frac{2\Delta_0 M_0^{*,3}}{\pi^2} \int_0^{k_F/M_0^*} \frac{\zeta^2 d\zeta}{\sqrt{1 + \zeta^2}} + \frac{2\Delta_0 M_0^{*,2} k_F^2}{\pi^2 E_F^*} \frac{\partial}{\partial \rho} \frac{k_F}{M_0^*} \\ &= -\frac{3g_\sigma \rho_S^I}{M_0^*} \frac{\partial f_0}{\partial \rho} + \frac{2\Delta_0 M_0^{*,2} k_F^2}{\pi^2 E_F^*} \left( \frac{\pi^2}{2M_0^* k_F^2} + \frac{g_\sigma k_F}{M_0^{*,2}} \frac{\partial f_0}{\partial \rho} \right) \\ &= -\frac{3g_\sigma \rho_S^I}{M_0^*} \frac{\partial f_0}{\partial \rho} + \frac{\Delta_0 M_0^*}{E_F^*} + \frac{3\Delta_0 g_\sigma \rho}{E_F^*} \frac{\partial f_0}{\partial \rho} = -3g_\sigma \left( \frac{\rho_S^I}{M_0^*} - \frac{\Delta_0 \rho}{E_F^*} \right) \frac{\partial f_0}{\partial \rho} + \frac{\Delta_0 M_0^*}{E_F^*}. \quad (\text{B3})\end{aligned}$$

The following two relations are useful in the derivations,

$$\frac{\partial k_F}{\partial \rho} = \frac{\pi^2}{2k_F^2}, \quad \frac{\partial E_F^*}{\partial \rho} = \frac{\pi^2}{2k_F E_F^*} - \frac{g_\sigma M_0^*}{E_F^*} \frac{\partial f_0}{\partial \rho}. \quad (\text{B4})$$

Similarly,

$$\begin{aligned}
\frac{\partial \rho_S^{\text{II}}}{\partial \rho} &= \frac{2C_0}{\pi^2} \frac{\partial}{\partial \rho} \frac{k_F^4}{M_0^*} \int_{k_F/M_0^*}^{p_F/M_0^*} \frac{d\zeta}{\zeta^2 \sqrt{1+\zeta^2}} + \frac{2C_0 k_F^4}{\pi^2 M_0^*} \frac{\partial}{\partial \rho} \int_{k_F/M_0^*}^{p_F/M_0^*} \frac{d\zeta}{\zeta^2 \sqrt{1+\zeta^2}} \\
&= \left( \frac{4}{k_F} \frac{\partial k_F}{\partial \rho} - \frac{1}{M_0^*} \frac{\partial M_0^*}{\partial \rho} \right) \frac{2C_0 k_F^4}{\pi^2 M_0^*} \int_{k_F/M_0^*}^{p_F/M_0^*} \frac{d\zeta}{\zeta^2 \sqrt{1+\zeta^2}} + \frac{2C_0 k_F^4}{\pi^2 M_0^*} \left[ \frac{M_0^{*,3}}{p_F^2 F_F^*} \frac{\partial}{\partial \rho} \left( \frac{p_F}{M_0^*} \right) - \frac{M_0^{*,3}}{k_F^2 E_F^*} \left( \frac{k_F}{M_0^*} \right) \right] \\
&= \frac{4\rho_S^{\text{II}}}{3\rho} + C_0 k_F^2 M_0^* \left( \frac{\phi_0}{p_F^2 F_F^*} - \frac{1}{k_F^2 E_F^*} \right) + g_\sigma \left[ \frac{\rho_S^{\text{II}}}{M_0^*} + \frac{2C_0 k_F^4}{\pi^2} \left( \frac{1}{p_F F_F^*} - \frac{1}{k_F E_F^*} \right) \right] \frac{\partial f_0}{\partial \rho}.
\end{aligned} \tag{B5}$$

Introducing,

$$\Phi = C_0 k_F^2 M_0^* \left( \frac{\phi_0}{p_F^2 F_F^*} - \frac{1}{k_F^2 E_F^*} \right), \quad \Psi = \frac{2C_0 k_F^4}{\pi^2} \left( \frac{1}{p_F F_F^*} - \frac{1}{k_F E_F^*} \right), \tag{B6}$$

then,

$$\frac{\partial \rho_S}{\partial \rho} = \frac{\partial f_0}{\partial \rho} \left[ g_\sigma \left( \frac{\rho_S^{\text{II}}}{M_0^*} + \Psi \right) - 3g_\sigma \left( \frac{\rho_S^{\text{I}}}{M_0^*} - \frac{\Delta_0 \rho}{E_F^*} \right) \right] + \frac{\Delta_0 M_0^*}{E_F^*} + \frac{4\rho_S^{\text{II}}}{3\rho} + \Phi. \tag{B7}$$

According to the equation of motion of  $f_0$ , we have

$$m_\sigma^2 \frac{\partial f_0}{\partial \rho} = g_\sigma \frac{\partial \rho_S}{\partial \rho} - 2b_\sigma M g_\sigma^3 f_0 \frac{\partial f_0}{\partial \rho} - 3c_\sigma g_\sigma^4 f_0^2 \frac{\partial f_0}{\partial \rho}. \tag{B8}$$

Thus we obtain the following expression for  $\partial f_0 / \partial \rho$

$$\frac{\partial f_0}{\partial \rho} = \frac{g_\sigma}{R_\sigma} \left( \frac{\Delta_0 M_0^*}{E_F^*} + \frac{4\rho_S^{\text{II}}}{3\rho} + \Phi \right), \tag{B9}$$

with

$$R_\sigma = m_\sigma^2 + 3g_\sigma^2 \left( \frac{\rho_S^{\text{I}}}{M_0^*} - \frac{\Delta_0 \rho}{E_F^*} \right) + 2b_\sigma M g_\sigma^3 f_0 + 3c_\sigma g_\sigma^4 f_0^2 - g_\sigma^2 \left( \frac{\rho_S^{\text{II}}}{M_0^*} + \Psi \right). \tag{B10}$$

By taking derivatives term by term in the kinetic symmetry energy of (24), we obtain the following kinetic slope

parameter

$$\begin{aligned}
L^{\text{kin}}(\rho) = & \left[ \frac{k_F^2 (E_F^{*,2} + M_0^{*,2})}{6E_F^{*,3}} + \frac{g_\sigma k_F^2 M_0^* \rho}{2E_F^{*,3}} \frac{\partial f_0}{\partial \rho} \right] \left[ 1 - 3C_0 \left( 1 - \frac{1}{\phi_0} \right) \right] \\
& - \frac{9\rho}{E_F^*} \left( \frac{\pi^2}{2k_F} - g_\sigma M_0^* \frac{\partial f_0}{\partial \rho} \right) C_0 \left[ C_1 \left( 1 - \frac{1}{\phi_0} \right) + \frac{\phi_1}{\phi_0} \right] \\
& - \frac{9C_0 \phi_1 (C_1 - \phi_1)}{4\pi^2 k_F \phi_0 E_F^*} \left[ \sqrt{1 + \theta^2} \text{arcsinh } \theta \left( \frac{3M_0^{*,5} \pi^2}{2k_F^2} + 4g_\sigma k_F M_0^{*,4} \frac{\partial f_0}{\partial \rho} \right) \right. \\
& \quad \left. + \frac{\pi^2}{2k_F^2} \left( 2k_F^5 - k_F^3 M_0^{*,2} - 3k_F M_0^{*,4} \right) - 4g_\sigma k_F^2 M_0^* E_F^{*,2} \frac{\partial f_0}{\partial \rho} \right] \\
& + \frac{2k_F C_0 (6C_1 + 1)}{3} \left[ \text{arcsinh}(\phi_0 \theta) - \sqrt{1 + \frac{1}{\phi_0^2 \theta^2}} - \text{arcsinh } \theta + \sqrt{1 + \frac{1}{\theta^2}} \right] \\
& + 2k_F \rho C_0 (6C_1 + 1) \left( \frac{M_0^* \pi^2}{2k_F^2} + g_\sigma k_F \frac{\partial f_0}{\partial \rho} \right) \\
& \quad \times \left( \frac{\phi_0}{F_F^* M_0^*} + \frac{M_0^*}{\phi_0^2 k_F^3 \sqrt{1 + \frac{1}{\phi_0^2 \theta^2}}} - \frac{1}{M_0^{*,2} \sqrt{1 + \theta^2}} - \frac{1}{M_0^* k_F \theta^2 \sqrt{1 + \frac{1}{\theta^2}}} \right) \\
& + \frac{3k_F C_0}{2} \left[ \frac{(1 + 3\phi_1)^2}{9} \left( \frac{\phi_0 k_F}{F_F^*} - \frac{2F_F^*}{\phi_0 k_F} \right) + \frac{2F_F^* (3\phi_1 - 1)}{9\phi_0 k_F} - \frac{1}{9} \frac{k_F}{E_F^*} + \frac{4E_F^*}{9k_F} \right] \\
& + \frac{9k_F \rho C_0}{2} \left( \frac{M_0^* \pi^2}{2k_F^2} + g_\sigma k_F \frac{\partial f_0}{\partial \rho} \right) \left[ \frac{(1 + 3\phi_1)^2}{9} \left( \frac{\phi_0}{F_F^* M_0^*} - \frac{\phi_0^3 \theta^2}{M_0^{*,2} (1 + \phi_0^2 \theta^2)^{3/2}} + \frac{2}{\phi_0 k_F^2 \sqrt{1 + \phi_0^2 \theta^2}} \right) \right. \\
& \quad \left. - \frac{2(3\phi_1 - 1)}{9\phi_0 k_F^2 \sqrt{1 + \phi_0^2 \theta^2}} - \frac{M_0^*}{9E_F^3} - \frac{4}{9k_F^2 \sqrt{1 + \theta^2}} \right] \\
& + \rho C_0 (4 + 3C_1) \left[ \frac{\pi^2}{2k_F^2} \left[ \frac{(1 + 3\phi_1) \phi_0 k_F}{M_0^* \sqrt{1 + \phi_0^2 \theta^2}} - \frac{k_F}{M_0^* \sqrt{1 + \theta^2}} \right] \right. \\
& \quad \left. - g_\sigma \frac{\partial f}{\partial \rho} \left[ \frac{(1 + 3\phi_1) \sqrt{1 + \phi_0^2 \theta^2}}{\phi_0} - \frac{(1 + 3\phi_1) \phi_0 k_F^2}{M_0^{*,2} \sqrt{1 + \phi_0^2 \theta^2}} - \sqrt{1 + \theta^2} + \frac{k_F^2}{M_0^{*,2} \sqrt{1 + \theta^2}} \right] \right], \quad (\text{B11})
\end{aligned}$$

where  $\partial f_0 / \partial \rho$  is given by (B9) and

$$\rho_S^{\text{I}} = \frac{\Delta_0 M_0^{*,3}}{\pi^2} \left( \theta \sqrt{1 + \theta^2} - \text{arcsinh } \theta \right), \quad \rho_S^{\text{II}} = \frac{2C_0 k_F^4}{\pi^2 M_0^*} \left( \sqrt{1 + \frac{1}{\theta^2}} - \sqrt{1 + \frac{1}{\phi_0^2 \theta^2}} \right), \quad (\text{B12})$$

with  $\theta = k_F / M_0^*$ . The potential part of the slope parameter of the symmetry energy is given by

$$L^{\text{pot}}(\rho) = 3\rho \frac{\partial E_{\text{sym}}^{\text{pot}}(\rho)}{\partial \rho} = \frac{3g_\rho^2 \rho}{2Q_\rho} - \frac{3g_\omega^3 g_\rho^4 \Lambda_V w_0 \rho^2}{Q_\omega Q_\rho^2} \quad (\text{B13})$$

with

$$Q_\omega = m_\omega^2 + 3c_\omega g_\omega^4 w_0 \quad (\text{B14})$$

and  $Q_\rho$  given by (28). The total slope parameter of the symmetry energy is given by

$$L(\rho) = L^{\text{kin}}(\rho) + L^{\text{pot}}(\rho). \quad (\text{B15})$$

### Appendix C: The Derivation of $K_0(\rho)$

The incompressibility coefficient  $K_0 \equiv K_0(\rho)$  can be obtained through

$$K_0(\rho) = 9\rho^2 \frac{\partial^2 E_0}{\partial \rho^2} = 9 \frac{\partial P_0}{\partial \rho} - \frac{18P_0}{\rho}, \quad (\text{C1})$$

where  $P_0(\rho)$  is the pressure of SNM. At normal density, the pressure of SNM is zero, thus only the first term of



the last expression is relevant for our aim. So we should first calculate the pressure  $P_0$  as a function of density. Before moving on, we first prove the following relation

$$P_0(\rho) = \rho^2 \frac{\partial E_0(\rho)}{\partial \rho} = \rho^2 \frac{\partial(\varepsilon_0/\rho)}{\partial \rho} \quad (\text{C2})$$

---

The EOS of SNM is obtained from the energy density

$$\varepsilon_0 = 2\varepsilon_{\varphi,0}^{\text{kin}} + \frac{1}{2}m_\sigma^2 f_0^2 + \frac{1}{2}m_\omega^2 w_0^2 + \frac{1}{3}b_\sigma M g_\sigma^3 f_0^3 + \frac{1}{4}c_\sigma g_\sigma^4 f_0^4 + \frac{3}{4}c_\omega g_\omega^4 w_0^4, \quad (\text{C3})$$

with

$$\varepsilon_{\varphi,0}^{\text{kin}} = \frac{2}{(2\pi)^3} \int_0^{\phi_0 k_F} n_{\mathbf{k}}^0 \sqrt{\mathbf{k}^2 + M_0^{*,2}} d\mathbf{k} = \frac{1}{\pi^2} \left[ \Delta_0 \int_0^{k_F} k^2 dk \sqrt{k^2 + M_0^{*,2}} + C_0 k_F^4 \int_{k_F}^{\phi_0 k_F} \frac{1}{k^2} \sqrt{k^2 + M_0^{*,2}} dk \right], \quad (\text{C4})$$

here  $\varphi$  is just a symbol reminding us that  $\varepsilon_{\varphi,0}^{\text{kin,I}} + \varepsilon_{\varphi,0}^{\text{kin,II}} = \varepsilon_{\varphi,0}^{\text{kin}} = 2^{-1}\varepsilon_0^{\text{kin}}$ , where  $\varepsilon_0^{\text{kin}}$  is the total kinetic energy density (including n and p). Similarly, the pressure is

$$P_0 = 2P_{\varphi,0}^{\text{kin}} - \frac{1}{2}m_\sigma^2 f_0^2 + \frac{1}{2}m_\omega^2 w_0^2 - \frac{1}{3}b_\sigma M g_\sigma^3 f_0^3 - \frac{1}{4}c_\sigma g_\sigma^4 f_0^4 + \frac{1}{4}c_\omega g_\omega^4 w_0^4, \quad (\text{C5})$$

with

$$P_{\varphi,0}^{\text{kin}} = \frac{1}{3\pi^2} \left[ \Delta_0 \int_0^{k_F} dk \frac{k^4}{\sqrt{k^2 + M_0^{*,2}}} + C_0 k_F^4 \int_{k_F}^{\phi_0 k_F} dk \frac{1}{\sqrt{k^2 + M_0^{*,2}}} \right]. \quad (\text{C6})$$

For the  $\omega$  field, we have  $\partial w_0 / \partial \rho = g_\omega / Q_\omega$ . The  $\omega$  part in the energy density has the following relation

$$\rho^2 \frac{\partial}{\partial \rho} \left( \frac{1}{2}m_\omega^2 w_0^2 + \frac{3}{4}c_\omega g_\omega^4 w_0^4 \right) = \frac{1}{2}m_\omega^2 w_0^2 + \frac{1}{4}c_\omega g_\omega^4 w_0^4, \quad (\text{C7})$$

which are just the corresponding terms of the pressure.

The proof for  $\sigma$  field is somewhat more complicated. The first part of the kinetic energy density is given by

$$\varepsilon_{\varphi,0}^{\text{kin,I}} = \frac{\Delta_0 M_0^{*,4}}{\pi^2} \int_0^{k_F/M_0^*} \zeta^2 \sqrt{1 + \zeta^2} d\zeta = \frac{\Delta_0 M_0^{*,4}}{\pi^2} \left[ \frac{1}{4}\theta(1 + \theta^2)^{3/2} - \frac{1}{8}\theta\sqrt{1 + \theta^2} - \frac{1}{8}\text{arcsinh}\theta \right], \quad (\text{C8})$$

thus

$$\begin{aligned} \frac{\partial \varepsilon_{\varphi,0}^{\text{kin,I}}}{\partial \rho} &= \frac{\Delta_0}{\pi^2} \cdot 4M_0^{*,3} \frac{\partial M_0^*}{\partial \rho} \int_0^{k_F/M_0^*} \zeta^2 \sqrt{1 + \zeta^2} d\zeta + \frac{\Delta_0 M_0^{*,4}}{\pi^2} \frac{\partial}{\partial \rho} \int_0^{k_F/M_0^*} \zeta^2 \sqrt{1 + \zeta^2} d\zeta \\ &= \frac{4\varepsilon_{\varphi,0}^{\text{kin,I}}}{M_0^*} \frac{\partial M_0^*}{\partial \rho} + \frac{\Delta_0 M_0^{*,4}}{\pi^2} \cdot \frac{k_F^2}{M_0^{*,3}} \frac{E_F^*}{M_0^{*,2}} \left( M_0^* \frac{\partial k_F}{\partial \rho} - k_F \frac{\partial M_0^*}{\partial \rho} \right) \\ &= \frac{4\varepsilon_{\varphi,0}^{\text{kin,I}}}{M_0^*} \frac{\partial M_0^*}{\partial \rho} + \frac{\Delta_0 k_F^2 E_F^*}{\pi^2 M_0^*} \left( M_0^* \frac{\partial k_F}{\partial \rho} - k_F \frac{\partial M_0^*}{\partial \rho} \right) \\ &= \left( \frac{4\varepsilon_{\varphi,0}^{\text{kin,I}}}{M_0^*} \frac{\partial M_0^*}{\partial \rho} - \frac{\Delta_0 k_F^3 E_F^*}{\pi^2 M_0^*} \right) \frac{\partial M_0^*}{\partial \rho} + \frac{\Delta_0 k_F^2 E_F^*}{\pi^2} \frac{\partial k_F}{\partial \rho} \\ &= \left( \frac{4\varepsilon_{\varphi,0}^{\text{kin,I}}}{M_0^*} \frac{\partial M_0^*}{\partial \rho} - \frac{\Delta_0 k_F^3 E_F^*}{\pi^2 M_0^*} \right) \frac{\partial M_0^*}{\partial \rho} + \frac{\Delta_0 E_F^*}{2}. \end{aligned} \quad (\text{C9})$$

Similarly,

$$\varepsilon_{\varphi,0}^{\text{kin,II}} = \frac{C_0 k_F^4}{\pi^2} \int_{k_F/M_0^*}^{\phi_0 k_F} \frac{\sqrt{1 + \zeta^2}}{\zeta^2} d\zeta = \frac{C_0 k_F^4}{\pi^2} \left[ \text{arcsinh}(\phi_0 \theta) - \text{arcsinh}\theta - \sqrt{1 + \frac{1}{\phi_0^2 \theta^2}} + \sqrt{1 + \frac{1}{\theta^2}} \right], \quad (\text{C10})$$

by calculating the quantities on both sides and then comparing them.

and

$$\begin{aligned} \frac{\partial \varepsilon_{\varnothing,0}^{\text{kin},\text{II}}}{\partial \rho} &= \frac{C_0}{\pi^2} \cdot 4k_F^3 \frac{\partial k_F}{\partial \rho} \int_{k_F/M_0^*}^{p_F/M_0^*} \frac{\sqrt{1+\zeta^2}}{\zeta^2} d\zeta + \frac{C_0 k_F^4}{\pi^2} \frac{\partial}{\partial \rho} \int_{k_F/M_0^*}^{p_F/M_0^*} \frac{\sqrt{1+\zeta^2}}{\zeta^2} d\zeta \\ &= \left[ \frac{4\varepsilon_{\varnothing,0}^{\text{kin},\text{II}}}{k_F} + \frac{C_0 k_F^4}{\pi^2} \left( \frac{\phi_0 F_F^*}{p_F^2} - \frac{E_F^*}{k_F^2} \right) \right] \frac{\partial k_F}{\partial \rho} - \frac{C_0 k_F^4}{\pi^2} \frac{1}{M_0^*} \left( \frac{F_F^*}{p_F} - \frac{E_F^*}{k_F} \right) \frac{\partial M_0^*}{\partial \rho}. \end{aligned} \quad (\text{C11})$$

Putting into the expression for  $\varepsilon_{\varnothing,0}^{\text{kin},\text{II}}$ , we have

$$\begin{aligned} \frac{\partial \varepsilon_{\varnothing,0}^{\text{kin},\text{II}}}{\partial \rho} &= \frac{4}{k_F} \frac{\partial k_F}{\partial \rho} \left[ \text{arcsinh}(\phi_0 \theta) - \text{arcsinh} \theta - \sqrt{1 + \frac{1}{\phi_0^2 \theta^2}} + \sqrt{1 + \frac{1}{\theta^2}} \right] \\ &\quad + \frac{C_0 k_F^4}{\pi^2} \left( \frac{\phi_0 F_F^*}{p_F^2} - \frac{E_F^*}{k_F^2} \right) \frac{\partial k_F}{\partial \rho} - \frac{C_0 k_F^4}{\pi^2} \frac{1}{M_0^*} \left( \frac{F_F^*}{p_F} - \frac{E_F^*}{k_F} \right) \frac{\partial M_0^*}{\partial \rho}. \end{aligned} \quad (\text{C12})$$

Then we have (only the  $f_0$  field is considered here)

$$\begin{aligned} \rho^2 \frac{\partial}{\partial \rho} \left( \frac{\varepsilon_0^{f_0}}{\rho} \right) &= \rho \frac{\partial \varepsilon_0^{f_0}}{\partial \rho} - \varepsilon_0^{f_0} \\ &= -\frac{1}{2} m_\sigma^2 f_0^2 - \frac{1}{3} b_\sigma M g_\sigma^3 f_0^3 - \frac{1}{4} c_\sigma g_\sigma^4 f_0^4 + \rho \frac{\partial f_0}{\partial \rho} (m_\sigma^2 f_0 + b_\sigma M g_\sigma^3 f_0^2 + c_\sigma g_\sigma^4 f_0^3) \\ &\quad - 2 \left[ \frac{\Delta_0 M_0^{*,4}}{\pi^2} \left[ \frac{1}{4} \theta (1 + \theta^2)^{3/2} - \frac{1}{8} \theta \sqrt{1 + \theta^2} - \frac{1}{8} \text{arcsinh} \theta \right] \right. \\ &\quad \left. + \frac{C_0 k_F^4}{\pi^2} \left[ \text{arcsinh}(\phi_0 \theta) - \text{arcsinh} \theta - \sqrt{1 + \frac{1}{\phi_0^2 \theta^2}} + \sqrt{1 + \frac{1}{\theta^2}} \right] \right] \\ &\quad + 2\rho \left[ -g_\sigma \frac{\partial f_0}{\partial \rho} \left( \frac{4\varepsilon_{\varnothing,0}^{\text{kin},\text{I}}}{M_0^*} - \frac{\Delta_0 k_F^3 E_F^*}{\pi^2 M_0^*} \right) + \frac{\Delta_0 E_F^*}{2} \right. \\ &\quad \left. + \left[ \frac{4\varepsilon_{\varnothing,0}^{\text{kin},\text{II}}}{k_F} + \frac{C_0 k_F^4}{\pi^2} \left( \frac{\phi_0 F_F^*}{p_F^2} - \frac{E_F^*}{k_F^2} \right) \right] \frac{\partial k_F}{\partial \rho} + \frac{g_\sigma}{M_0^*} \frac{C_0 k_F^4}{\pi^2} \left( \frac{F_F^*}{p_F} - \frac{E_F^*}{k_F} \right) \frac{\partial f_0}{\partial \rho} \right]. \end{aligned}$$

The term proportional to  $\partial f_0 / \partial \rho$  in  $\rho^2 \partial(\varepsilon_0 / \rho) / \partial \rho$  is

$$\Pi_0 = \rho (m_\sigma^2 f_0 + b_\sigma M g_\sigma^3 f_0^2 + c_\sigma g_\sigma^4 f_0^3) - 2g_\sigma \rho \left( \frac{4\varepsilon_{\varnothing,0}^{\text{kin},\text{I}}}{M_0^*} - \frac{\Delta_0 k_F^3 E_F^*}{\pi^2 M_0^*} \right) + \frac{2g_\sigma \rho}{M_0^*} \frac{C_0 k_F^4}{\pi^2} \left( \frac{F_F^*}{p_F} - \frac{E_F^*}{k_F} \right), \quad (\text{C13})$$

where

$$\varepsilon_{\varnothing,0}^{\text{kin},\text{I}} = \frac{\Delta_0 k_F^3 E_F^*}{4\pi^2} + \frac{M_0^* \rho_{\text{S},\varnothing,0}^{\text{I}}}{4}, \quad \frac{4\varepsilon_{\varnothing,0}^{\text{kin},\text{I}}}{M_0^*} - \frac{\Delta_0 k_F^3 E_F^*}{\pi^2 M_0^*} = \rho_{\text{S},\varnothing,0}^{\text{I}}, \quad (\text{C14})$$

Similarly, we have

$$\rho_{\text{S},\varnothing,0}^{\text{II}} = -\frac{C_0 k_F^4}{\pi^2 M_0^*} \left( \frac{F_F^*}{p_F} - \frac{E_F^*}{k_F} \right), \quad (\text{C15})$$

thus

$$\Pi_0 = \rho (m_\sigma^2 f_0 + b_\sigma M g_\sigma^3 f_0^2 + c_\sigma g_\sigma^4 f_0^3) - 2g_\sigma \rho_{\text{S},\varnothing,0}^{\text{I}} - 2g_\sigma \rho_{\text{S},\varnothing,0}^{\text{II}} = \rho [(m_\sigma^2 f_0 + b_\sigma M g_\sigma^3 f_0^2 + c_\sigma g_\sigma^4 f_0^3) - g_\sigma \rho_{\text{S}}], \quad (\text{C16})$$

where  $\rho_{\text{S}} = 2(\rho_{\text{S},\varnothing,0}^{\text{I}} + \rho_{\text{S},\varnothing,0}^{\text{II}})$  is the total scalar density, the above equation equals to zero according to the equation

of motion of  $f_0$ . Thus

$$\begin{aligned} \rho^2 \frac{\partial}{\partial \rho} \left( \frac{\varepsilon_0^{f_0}}{\rho} \right) = & -\frac{1}{2} m_\sigma^2 f_0^2 - \frac{1}{3} b_\sigma M g_\sigma^3 f_0^3 - \frac{1}{4} c_\sigma g_\sigma^4 f_0^4 \\ & - 2 \left[ \frac{\Delta_0 M_0^{*,4}}{\pi^2} \left[ \frac{1}{4} \theta (1 + \theta^2)^{3/2} - \frac{1}{8} \theta \sqrt{1 + \theta^2} - \frac{1}{8} \operatorname{arcsinh} \theta \right] \right. \\ & + \frac{C_0 k_F^4}{\pi^2} \left[ \operatorname{arcsinh}(\phi_0 \theta) - \operatorname{arcsinh} \theta - \sqrt{1 + \frac{1}{\phi_0^2 \theta^2}} + \sqrt{1 + \frac{1}{\theta^2}} \right] \\ & \left. + 2\rho \left[ \frac{\Delta_0 E_F^*}{2} + \left[ \frac{4\varepsilon_{\varnothing,0}^{\text{kin,II}}}{k_F} + \frac{C_0 k_F^4}{\pi^2} \left( \frac{\phi_0 F_F^*}{p_F^2} - \frac{E_F^*}{k_F^2} \right) \right] \frac{\partial k_F}{\partial \rho} \right] \right]. \end{aligned} \quad (\text{C17})$$

The expression for pressure is easy to obtain,

$$P_{\varnothing,0}^{\text{kin,I}} = \frac{\Delta_0 M_0^{*,4}}{3\pi^2} \int_0^{k_F/M_0^*} \frac{\zeta^4 d\zeta}{\sqrt{1 + \zeta^2}} = \frac{\Delta_0 M_0^{*,4}}{3\pi^2} \left[ \frac{1}{4} \theta^3 \sqrt{1 + \theta^2} - \frac{3}{8} \theta \sqrt{1 + \theta^2} + \frac{3}{8} \operatorname{arcsinh} \theta \right], \quad (\text{C18})$$

$$P_{\varnothing,0}^{\text{kin,II}} = \frac{C_0 k_F^4}{3\pi^2} \int_{k_F/M_0^*}^{p_F/M_0^*} \frac{d\zeta}{\sqrt{1 + \zeta^2}} = \frac{C_0 k_F^4}{3\pi^2} [\operatorname{arcsinh}(\phi_0 \theta) - \operatorname{arcsinh} \theta], \quad (\text{C19})$$

thus

$$\begin{aligned} P_0^{f_0} = & -\frac{1}{2} m_\sigma^2 f_0^2 - \frac{1}{3} b_\sigma M g_\sigma^3 f_0^3 - \frac{1}{4} c_\sigma g_\sigma^4 f_0^4 \\ & + \frac{2\Delta_0 M_0^{*,4}}{3\pi^2} \left[ \frac{1}{4} \theta^3 \sqrt{1 + \theta^2} - \frac{3}{8} \theta \sqrt{1 + \theta^2} + \frac{3}{8} \operatorname{arcsinh} \theta \right] \\ & + \frac{2C_0 k_F^4}{3\pi^2} [\operatorname{arcsinh}(\phi_0 \theta) - \operatorname{arcsinh} \theta]. \end{aligned} \quad (\text{C20})$$

It is obvious that the first line of (C17) and that of (C20) are the same. Terms proportional to  $\Delta_0$  in (C17) are

$$\begin{aligned} & \Delta_0 \rho E_F^* - \frac{2\Delta_0 M_0^{*,4}}{\pi^2} \left[ \frac{1}{4} \theta (1 + \theta^2)^{3/2} - \frac{1}{8} \theta \sqrt{1 + \theta^2} - \frac{1}{8} \operatorname{arcsinh} \theta \right] \\ = & \frac{2\Delta_0 k_F^3 E_F^*}{3\pi^2} - \frac{2\Delta_0 M_0^{*,4}}{\pi^2} \left[ \frac{1}{4} \theta (1 + \theta^2)^{3/2} - \frac{1}{8} \theta \sqrt{1 + \theta^2} - \frac{1}{8} \operatorname{arcsinh} \theta \right] \\ = & \frac{2\Delta_0 M_0^{*,4}}{3\pi^2} \left[ \frac{1}{4} \theta^3 \sqrt{1 + \theta^2} - \frac{3}{8} \theta \sqrt{1 + \theta^2} + \frac{3}{8} \operatorname{arcsinh} \theta \right], \end{aligned} \quad (\text{C21})$$

this is the corresponding term in the pressure proportional to  $\Delta_0$ . Similarly, the remaining terms in (C17) are

$$\begin{aligned} & 2\rho \frac{\partial k_F}{\partial \rho} \left[ \frac{4\varepsilon_{\varnothing,0}^{\text{kin,II}}}{k_F} + \frac{C_0 k_F^4}{\pi^2} \left( \frac{\phi_0 F_F^*}{p_F^2} - \frac{E_F^*}{k_F^2} \right) \right] \\ = & \frac{2C_0 k_F^4}{3\pi^2} \left[ 4 \left( \operatorname{arcsinh}(\phi_0 \theta) - \operatorname{arcsinh} \theta - \sqrt{1 + \frac{1}{\phi_0^2 \theta^2}} + \sqrt{1 + \frac{1}{\theta^2}} \right) + \left( \sqrt{1 + \frac{1}{\phi_0^2 \theta^2}} - \sqrt{1 + \frac{1}{\theta^2}} \right) \right]. \end{aligned} \quad (\text{C22})$$

and (i.e., the third line of (C17))

$$-\frac{2C_0 k_F^4}{3\pi^2} \cdot 3 \left( \operatorname{arcsinh}(\phi_0 \theta) - \operatorname{arcsinh} \theta - \sqrt{1 + \frac{1}{\phi_0^2 \theta^2}} + \sqrt{1 + \frac{1}{\theta^2}} \right), \quad (\text{C23})$$

combining (C22) and (C23), we obtain the following expression proportional to  $C_0$  in (C17),

$$\frac{2C_0 k_F^4}{3\pi^2} [\operatorname{arcsinh}(\phi_0 \theta) - \operatorname{arcsinh} \theta], \quad (\text{C24})$$

which is exactly the same as the last line of (C20). Thus we have proved the relation (C2).

The expression for pressure including  $w_0$  field then reads

$$\begin{aligned}
P_0 = & -\frac{1}{2}m_\sigma^2 f_0^2 - \frac{1}{3}b_\sigma M g_\sigma^3 f_0^3 - \frac{1}{4}c_\sigma g_\sigma^4 f_0^4 + \frac{1}{2}m_\omega^2 w_0^2 + \frac{1}{4}c_\omega g_\omega^4 w_0^4 \\
& + \frac{2\Delta_0 M_0^{*,4}}{3\pi^2} \left[ \frac{1}{4}\theta^3 \sqrt{1+\theta^2} - \frac{3}{8}\theta \sqrt{1+\theta^2} + \frac{3}{8}\text{arcsinh}\theta \right] \\
& + \frac{2C_0 k_F^4}{3\pi^2} [\text{arcsinh}(\phi_0 \theta) - \text{arcsinh}\theta].
\end{aligned} \tag{C25}$$

The contribution to  $K_0$  from  $w_0$  field is

$$9 \frac{\partial}{\partial \rho} \left( \frac{1}{2}m_\omega^2 w_0^2 + \frac{1}{4}c_\omega g_\omega^4 w_0^4 \right) = \frac{9\rho g_\omega^2}{Q_\omega}. \tag{C26}$$

For the  $f_0$  field, we have

$$\begin{aligned}
\frac{\partial P_0^{f_0}}{\partial \rho} = & -f_0 \frac{\partial f_0}{\partial \rho} (m_\sigma^2 + b_\sigma M g_\sigma^3 f_0 + c_\sigma g_\sigma^4 f_0^2) + \frac{2\Delta_0}{3\pi^2} \left[ W(\theta) \frac{\partial M_0^{*,4}}{\partial \rho} + M_0^{*,4} \frac{\partial W(\theta)}{\partial \rho} \right] + \frac{2C_0}{3\pi^2} \left[ V(\theta) \frac{\partial k_F^4}{\partial \rho} + k_F^4 \frac{\partial V(\theta)}{\partial \rho} \right] \\
= & -\frac{\partial f_0}{\partial \rho} \left[ f_0 (m_\sigma^2 + b_\sigma M g_\sigma^3 f_0 + c_\sigma g_\sigma^4 f_0^2) + \frac{8g_\sigma \Delta_0 M_0^{*,3} W(\theta)}{3\pi^2} \right] + \frac{4C_0 k_F V(\theta)}{3} \\
& + \left[ \frac{2\Delta_0 k_F^4}{3\pi^2 M_0^* E_F^*} + \frac{2C_0 k_F^4}{3\pi^2 M_0^*} \left( \frac{\phi_0}{F_F^*} - \frac{1}{E_F^*} \right) \right] \left( M_0^* \frac{\partial k_F}{\partial \rho} - k_F \frac{\partial M_0^*}{\partial \rho} \right),
\end{aligned} \tag{C27}$$

where

$$W(\theta) = \frac{1}{4}\theta^3 \sqrt{1+\theta^2} - \frac{3}{8}\theta \sqrt{1+\theta^2} + \frac{3}{8}\text{arcsinh}\theta, \quad V(\theta) = \text{arcsinh}(\phi_0 \theta) - \text{arcsinh}\theta. \tag{C28}$$

The corresponding contribution to the  $K_0$  of  $f_0$  field is

$$\begin{aligned}
& -9 \frac{\partial f_0}{\partial \rho} \left[ f_0 (m_\sigma^2 + b_\sigma M g_\sigma^3 f_0 + c_\sigma g_\sigma^4 f_0^2) + \frac{8g_\sigma \Delta_0 M_0^{*,3} W(\theta)}{3\pi^2} \right] + 12C_0 k_F V(\theta) \\
& + 9 \left[ \frac{2\Delta_0 k_F^4}{3\pi^2 M_0^* E_F^*} + \frac{2C_0 k_F^4}{3\pi^2 M_0^*} \left( \frac{\phi_0}{F_F^*} - \frac{1}{E_F^*} \right) \right] \left( M_0^* \frac{\partial k_F}{\partial \rho} - k_F \frac{\partial M_0^*}{\partial \rho} \right).
\end{aligned} \tag{C29}$$

Combining the above results, we finally obtain the expression for  $K_0(\rho)$  as

$$\begin{aligned}
K_0(\rho) = & -9 \frac{\partial f_0}{\partial \rho} \left[ f_0 (m_\sigma^2 + b_\sigma M g_\sigma^3 f_0 + c_\sigma g_\sigma^4 f_0^2) + \frac{8g_\sigma \Delta_0 M_0^{*,3} W(\theta)}{3\pi^2} \right] \\
& + 9 \left[ \frac{2\Delta_0 k_F^4}{3\pi^2 M_0^* E_F^*} + \frac{2C_0 k_F^4}{3\pi^2 M_0^*} \left( \frac{\phi_0}{F_F^*} - \frac{1}{E_F^*} \right) \right] \left( \frac{M_0^* \pi^2}{2k_F^2} + g_\sigma k_F \frac{\partial f_0}{\partial \rho} \right) \\
& + 12C_0 k_F V(\theta) + \frac{9\rho g_\omega^2}{Q_\omega} - \frac{18P_0}{\rho},
\end{aligned} \tag{C30}$$

with  $\partial f_0/\partial \rho$  given by (B9) and  $P_0$  by (C25).

- 
- [1] “Topical issue on nuclear symmetry energy”, Eds., B.A. Li, A. Ramos, G. Verde, and I. Vidaña, Eur. Phys. J. A **50**, No. 2, (2014).  
[2] B.A. Li, C.M. Ko, and W. Bauer, Int. J. Mod. Phys. E

- 7**, 147 (1998).  
[3] P. Danielewicz, R. Lacey, and W.G. Lynch, Science **298**, 1592 (2002).  
[4] V. Baran, M. Colonna, V. Greco, and M. Di Toro, Phys.



- Rep. **410**, 335 (2005).
- [5] A.W. Steiner, M. Prakash, J.M. Lattimer, and P.J. Ellis, Phys. Rep. **411**, 325 (2005).
  - [6] L.W. Chen, C.M. Ko, B.A. Li, and G.C. Yong, Front. Phys. China **2**, 327 (2007).
  - [7] B.A. Li, L.W. Chen, and C.M. Ko, Phys. Rep. **464**, 113 (2008).
  - [8] B.M. Tsang *et al.*, Phys. Rev. C **86**, 105803 (2012).
  - [9] L.W. Chen, C.M. Ko, B.A. Li, C. Xu, and J. Xu, Eur. Phys. J. A **50**, 29 (2014).
  - [10] N.K. Glendenning, Compact Stars, 2nd edition, Springer-Verlag New York, Inc., 2000.
  - [11] J.M. Lattimer and M. Prakash, Science **304**, 536 (2004); Phys. Rep. **442**, 109 (2007).
  - [12] J.M. Lattimer, Annu. Rev. Nucl. Part. Sci. **62**, 485 (2012).
  - [13] J.M. Lattimer and A.W. Steiner, Eur. Phys. J. A50, 40 (2014).
  - [14] C. Xu and B.A. Li, Phys. Rev. C81, 064612 (2010).
  - [15] Hyun Kyu Lee, Byung-Yoon Park and Mannque Rho, Phys. Rev. C83, 025206 (2011).
  - [16] Hyun Kyu Lee and Mannque Rho, Eur. Phys. J. A50, 14 (2014).
  - [17] Y.N. Wang, J.N. Hu, H. Toki and H. Shen, Progress of Theoretical Physics, Vol. 127 No. 4, 739 (2012).
  - [18] K. Hagel, J.B. Natowitz and G. Röpke, Euro. Phys. J. A50, 39 (2014).
  - [19] S. Typel, H.H. Wolter, G. Röpke and D. Blaschke, Eur. Phys. J. A50, 17 (2014).
  - [20] J. Margueron, E. Khan, G. Colo, K. Hagino and H. Sagawa, Eur. Phys. J. A50, 18 (2014).
  - [21] H.A. Bethe, Ann. Rev. Nucl. Part. Sci. 21, 93 (1971).
  - [22] A.N. Antonov, P.E. Hodgson, and I.Zh. Petkov, Nucleon Momentum and Density Distribution in Nuclei, Clarendon Press, Oxford, 1988.
  - [23] J. Arrington, D.W. Higinbotham, G. Rosner, and M. Sargsian, Prog. Part. Nucl. Phys. **67**, 898 (2012).
  - [24] C. Ciofi degli Atti, Phys. Rep. **590**, 1 (2015).
  - [25] R. Weiss, B. Bazak, and N. Barnea, Phys. Rev. Lett. **114**, 012501 (2015).
  - [26] R. Weiss, B. Bazak, and N. Barnea, arXiv:1503.07047.
  - [27] O. Hen *et al.*, Science **346**, 614 (2015).
  - [28] O. Hen, L.B. Weinstein, E. Piasetzky, G.A. Miller, M. Sargsian, and Y. Sagi, arXiv:1407.8175.
  - [29] C. Colle, O. Hen, W. Cosyn, I. Korover, E. Piasetzky, J. Ryckebusch, and L.B. Weinstein, Phys. Rev. C **92**, 024604 (2015).
  - [30] K.S. Egiyan *et al.*, Phys. Rev. Lett. **96**, 082501 (2006); E. Piasetzky *et al.*, Phys. Rev. Lett. **97**, 162504 (2006); R. Shneor *et al.*, Phys. Rev. Lett. **99**, 072501 (2007); R. Subedi *et al.*, Science **320**, 1467 (2008); L.B. Weinstein *et al.*, Phys. Rev. Lett. **106**, 052301 (2011); I. Korover *et al.*, Phys. Rev. Lett. **113**, 022501 (2014).
  - [31] C. Xu and B.A. Li, arXiv: 1104.2075.
  - [32] C. Xu, A. Li, B.A. Li, J. of Phys: Conference Series **420**, 012190 (2013).
  - [33] I. Vidaña, A. Polls, and C. Providência, Phys. Rev. C **84**, 062801(R) (2011).
  - [34] A. Lovato, O. Benhar, S. Fantoni, A.Yu. Illarionov, and K.E. Schmidt, Phys. Rev. C **83**, 054003 (2011).
  - [35] A. Carbone, A. Polls, A. Rios, Eur. Phys. Lett. **97**, 22001 (2012).
  - [36] A. Rios, A. Polls, and W.H. Dickhoff, Phys. Rev. C **89**, 044303 (2014).
  - [37] A. Carbone, A. Polls, C. Providência, A. Rios, and I. Vidaña, Eur. Phys. A, (2014) 50: 13
  - [38] O. Hen, B.A. Li, W.J. Guo, L.B. Weinstein, and E. Piasetzky, Phys. Rev. C **91**, 025803 (2015).
  - [39] B.J. Cai and B.A. Li, Phys. Rev. C **92**, 011601(R) (2015).
  - [40] B.A. Li and X. Han, Phys. Lett. **B727**, 276 (2013).
  - [41] B.A. Li, W.J. Guo, and Z.Z. Shi, Phys. Rev. C **91**, 044601 (2015).
  - [42] G.C. Yong, arXiv: 1503.08523.
  - [43] B.A. Li, Phys. Rev. C **92**, 034603 (2015).
  - [44] B.J. Cai, F.J. Fattoyev, B.A. Li, and W.G. Newton, Phys. Rev. C **92**, 015802 (2015).
  - [45] A. Drago, A. Lavagno, G. Pagliara, and D. Pigato, Phys. Rev. C **90**, 065809 (2014).
  - [46] A. Schwenk and C.J. Pethick, Phys. Rev. Lett. **95**, 160401 (2005).
  - [47] E. Epelbaum, H. Krebs, D. Lee, and Ulf-G. Meissner, Eur. Phys. A **40**, 199 (2009).
  - [48] I. Tews, T. Krüger, K. Hebeler, and A. Schwenk, Phys. Rev. Lett. **110**, 032504 (2013); T. Krüger, I. Tews, K. Hebeler, and A. Schwenk, Phys. Rev. C **88**, 025802 (2013).
  - [49] A. Gezerlis *et al.*, Phys. Rev. Lett. **111**, 032501 (2013).
  - [50] A. Gezerlis and J. Carlson, Phys. Rev. C **81**, 025803 (2010).
  - [51] S.N. Tan, Ann. Phys. **323**, 2952 (2008); **323**, 2971 (2008); **323**, 2987 (2008).
  - [52] J.T. Stewart *et al.*, Phys. Rev. Lett. **104**, 235301 (2010); E.D. Kuhnle *et al.*, Phys. Rev. Lett. **105**, 070402 (2010).
  - [53] P. Ring, Prog. Part. Nucl. Phys. **37**, 193 (1996).
  - [54] B.D. Serot and J.D. Walecka, Adv. Nucl. Phys. **16**, 1 (1986).
  - [55] B.D. Serot and J.D. Walecka, Int. J. Mod. Phys. E **6**, 515 (1997).
  - [56] P.-G. Reinhard, Rep. Prog. Phys. **52**, 439 (1989).
  - [57] J. Meng, H. Toki, S.G. Zhou, S.G. Zhang, W.H. Long, and L.S. Geng, Prog. Part. Nucl. Phys. **57**, 470 (2006).
  - [58] F.J. Fattoyev, C.J. Horowitz, J. Piekarewicz, and G. Shen, Phys. Rev. C **82**, 055803 (2010).
  - [59] F.J. Fattoyev, J. Carvajal, W.G. Newton, and B.A. Li, Phys. Rev. C **87**, 015806 (2013).
  - [60] M. Dutra, *et al.*, Phys. Rev. C **90**, 055203 (2014).
  - [61] H. Müller and B.D. Serot, Nucl. Phys. **A606**, 508 (1996).
  - [62] C.J. Horowitz and J. Piekarewicz, 2001, Phys. Rev. Lett. **86**, 5647 (2001).
  - [63] C.J. Horowitz and J. Piekarewicz, 2001a, Phys. Rev. C **64**, 062802(R) (2001).
  - [64] C.J. Horowitz and J. Piekarewicz, 2002, Phys. Rev. C **66**, 055803 (2002).
  - [65] B.G. Todd-Rutel and J. Piekarewicz, 2005, Phys. Rev. Lett. **95**, 122501 (2005).
  - [66] L.W. Chen, C.M. Ko, and B.A. Li, 2007, Phys. Rev. C **76**, 054316 (2007).
  - [67] B.J. Cai and L.W. Chen, 2012, Phys. Rev. C **85**, 024302 (2012).
  - [68] D.H. Youngblood, H.L. Clark, and Y.-W. Lui, Phys. Rev. Lett. **82**, 691 (1999).
  - [69] S. Shlomo, V.M. Kolomietz, and G. Colò, Eur. Phys. J. A **30**, 23 (2006).
  - [70] J. Piekarewicz, J. Phys. G **37**, 064038 (2010).
  - [71] L.W. Chen and J.Z. Gu, J. Phys. G **39**, 035104 (2012).
  - [72] G. Colò, U. Garg and H. Sagawa, Eur. Phys. J. A50, 26 (2014).
  - [73] L.W. Chen, B.J. Cai, C.M. Ko, B.A. Li, C. Shen, and J.

- Xu, Phys. Rev. C **80**, 014332 (2009).
- [74] L.W. Chen, 2011, Sci. China: Phys. Mech. Astron. 54, suppl., 1, s124 (2011) [arXiv:1101.2384].
  - [75] B.J. Cai and L.W. Chen, arXiv:1402.4242.
  - [76] M. Farine, J.M. Pearson and F. Tondeur, Nucl. Phys. **A615**, 135 (1997).
  - [77] A.W. Steiner, J.M. Lattimer, and E.F. Brown, Astrophys. J. **722**, 33 (2010).
  - [78] M. Meixner, J.P. Olson, G. Mathews, N.Q. Lan and H.E. Dalhed, arXiv:1303.0064.
  - [79] R. Sellaheewa and A. Rios, Phys. Rev. C **90**, 054327 (2014).
  - [80] B.M. Santos, M. Dutra, O. Lourenco, and A. Delfino, Phys. Rev. C **92**, 015210 (2015)
  - [81] M.M. Sargsian, Phys. Rev. C **89**, 034305 (2014); M.M. Sargsian, arXiv:1312.2263; M. McGauley and M.M. Sargsian, arXiv:1102.3973.
  - [82] M. Centelles, X.R. Maza, X. Viñas, and M. Warda, Phys. Rev. Lett. **102**, 122502 (2009).
  - [83] L.W. Chen, Phys. Rev. C **83**, 044308 (2011).
  - [84] X.R. Maza *et al.*, Phys. Rev. C **88**, 024316 (2013).
  - [85] W.D. Myers, and W.J. Swiatecki, Ann. Phys. **55**, 395 (1969).
  - [86] P. Danielewicz, Nucl. Phys. **A727**, 233 (2003).
  - [87] P. Danielewicz and J. Lee, Nucl. Phys. **A818**, 36 (2009).
  - [88] P. Danielewicz and J. Lee, Nucl. Phys. **A922**, 1 (2014).
  - [89] L. Lapikas, Nucl. Phys. A553, 297c (1993).
  - [90] Z. Zhang and L.W. Chen, Phys. Rev. C **92**, 031301(R) (2015).
  - [91] Z.G. Xiao, B.A. Li, L.W. Chen, G.C. Yong, and M. Zhang, Phys. Rev. Lett. **102**, 062502 (2009).
  - [92] L.L. Frankfurt, M. Sargsian, and M.I. Strikman, Int. Mod. Phys. A **23**, 2991 (2008).
  - [93] J.M. Dong, U. Lombardo, H.F. Zhang, and W. Zuo, arXiv:1512.02746.
  - [94] Henry Fleming, William G. Newton, Isaac Vidaña and Bao-An Li,  
<http://meetings.aps.org/link/BAPS.2015.TSF.F3.1>
  - [95] W.G. Newton and I. Vidaña, private communications.
  - [96] J. Xu, L.W. Chen, B.A. Li, and H.R. Ma, Phys. Rev. C **79**, 035802 (2009); Astrophys. J. **697**, 1549 (2009).
  - [97] J. Carriere, C. J. Horowitz, and J. Piekarewicz, Astrophys. J. **593**, 463 (2003).
  - [98] G. Baym, C. Pethick, and P. Sutherland, Astrophys. J. **170**, 299 (1971); K. Iida and K. Sato, Astrophys. J. **477**, 294 (1997).
  - [99] B.D. Serot, Phys. Lett. **B86**, 146 (1979).